Journal of Membrane Science 561 (2018) 39–58

Contents lists available at ScienceDirect

Journal of Membrane Science

journal homepage: www.elsevier.com/locate/memsci

A novel time lag method for the analysis of mixed gas diffusion in polymeric membranes by on-line mass spectrometry: Method development and validation

S.C. Fraga[a], M. Monteleone[b], M. Lanč[c], E. Esposito[b], A. Fuoco[b], L. Giorno[b], K. Pilnáček[c], K. Friess[c], M. Carta[d], N.B. McKeown[e], P. Izák[f], Z. Petrusová[f], J.G. Crespo[a], C. Brazinha[a,*], J.C. Jansen[b,*]

[a] LAQV/Requimte, Faculdade de Ciências e Tecnologia, Universidade Nova de Lisboa, Campus de Caparica, 2829-516 Caparica, Portugal
[b] Institute on Membrane Technology (ITM-CNR), Via P. Bucci 17/C, 87036 Rende, CS, Italy
[c] University of Chemistry and Technology, Department of Physical Chemistry, Technická 5, Prague 166 28, Czech Republic
[d] Department of Chemistry, College of Science, Swansea University, Grove Building, Singleton Park, SA2 8PP Swansea, United Kingdom
[e] EastChem, School of Chemistry, University of Edinburgh, David Brewster Road, EH9 3FJ, United Kingdom
[f] Institute of Chemical Process Fundamentals, Czech Academy of Sciences, v.v.i., Rozvojová 135, 165 02 Prague 6 – Suchdol, Czech Republic

ARTICLE INFO

Keywords:
Gas separation membrane
Mixed gas diffusion
Time lag method
Diffusion coefficient
On-line mass spectrometry

ABSTRACT

A novel method to determine the individual diffusion coefficients of gases in a mixture during their permeation through polymeric membranes is described. The method was developed in two independent laboratories, using rubbery Pebax® and glassy Hyflon® AD60X membrane samples as standards, and validated using the Tröger's base containing Polymer of Intrinsic Microporosity, PIM-EA-TB. Monitoring of the permeate composition in real time by a quadrupole mass spectrometer allowed the analysis of the permeation transient for gas mixtures. Two operation modes, either with a vacuum in the permeate and a direct connection to the mass spectrometer via a heated restriction, or using a sweeping gas and a heated capillary sample inlet, give excellent agreement with the traditional time lag method for single gases. A complete overview of the method development, identification of the critical parameters, instruments calibration, data elaboration and estimation of the experimental accuracy are provided. Validation with PIM-EA-TB, shows that the method can also successfully detect anomalous phenomena, related to pressure and concentration dependency of the transport properties, physical aging or penetrant-induced dilation. Rapid online analysis of the permeate composition makes the method also very suitable for routine mixed gas permeability measurements.

1. Introduction

In the search for more competitive technologies in terms of process economy, reduced environmental impact or energy consumption [1], membrane separations are emerging for various applications, like natural gas sweetening, biogas upgrading or carbon capture from flue gas or industrial waste gas. Increasingly challenging separation problems, involving particularly difficult olefin/paraffin separations or particularly voluminous flue gas and natural gas streams, has spurred the development of novel materials with improved selectivity and/or permeability [2]. Materials that have received considerable attention in the last 1–2 decades include glassy perfluoropolymers [3–5], polymers of intrinsic microporosity (PIMs) [6–10], microporous organic polymers (MOP) [10], thermally rearranged (TR) polymers [11–13], ionic liquids and poly(ionic liquid)s [14–16]. The development of such sophisticated novel membrane materials inevitably requires the development of improved methods to study their transport properties.

Since the transport in dense polymeric membranes is governed by the solution-diffusion mechanism, the most common approach to study their transport properties, is the so-called time lag method. It allows the determination of both the permeability coefficient and the diffusion coefficient of pure gases in the polymeric matrix, and indirectly, the solubility coefficient [17,18]. This is one of the simplest and most versatile methods for determination of the diffusion coefficient and it is applicable to porous media exhibiting surface diffusion or glassy polymers with strongly nonlinear sorption behaviour [19]. The feed pressure decay in pseudo-steady state conditions [20] or the simultaneous measurement of the feed pressure decay and the permeate pressure increase [21] were proposed to study the transport properties of materials with concentration dependent diffusion or with a strongly

* Corresponding authors.
E-mail addresses: c.brazinha@fct.unl.pt (C. Brazinha), johannescarolus.jansen@cnr.it (J.C. Jansen).

https://doi.org/10.1016/j.memsci.2018.04.029
Received 9 February 2018; Received in revised form 13 April 2018; Accepted 17 April 2018
Available online 24 April 2018

Abbreviations and symbols

Abbreviations

AMU	Atomic mass unit
BPC	Back pressure controller
GC	Gas chromatography
HFE	1-methoxy-perfluorobutane (mixture of n-butyl and iso-butyl isomers)
MFC	Mass flow controller
MIMS	Membrane inlet mass spectrometry or Membrane introduction mass spectrometry
MS	Mass Spectrometer, Mass Spectrometry
PC	Personal computer
PDMS	Polydimethylsiloxane
PI	Pressure indicator
PIM	Polymer of intrinsic microporosity
PPA	Partial pressure analyser
PTFE	Polytetrafluoroethylene
RGA	Residual gas analyser
SEM	Secondary Electron Multiplier
STP	Standard temperature and pressure
Vol	Volume
Wt	Weight

Symbols unit

A	Membrane area, m^2
c	Penetrant concentration, $mol\,m^{-3}$
D	Diffusion coefficient, $m^2\,s^{-1}$
I	Mass spectrometer signal intensity, Torr or mA
J	Flux, $cm^3_{STP}\,cm^{-2}\,s^{-1}$
l	Membrane thickness, m or μm
M	Molar mass, $g\,mol^{-1}$
p	Pressure or partial pressure, Torr or mbar
P	Permeability coefficient, Barrer or $m^3_{STP}\,m\,m^{-1}\,h^{-1}\,bar^{-1}$
Q	Amount of penetrant (in Eq. (30)), $mol\,m^{-2}$
Q	Volumetric flow rate, $cm^3_{STP}\,min^{-1}$
R	Universal gas constant, $8.314{\cdot}10^{-5}\,m^3\,bar\,mol^{-1}\,K^{-1}$
RS	Relative sensitivity/Relative sensitivity factor, (–)
S	Solubility, $m^3_{STP}\,m^{-3}\,bar^{-1}$
t	Time, s
T	Absolute temperature, K
V	Volume, cm^3 or m^3
x	Molar fraction, (–) or %
x	Number of analyses (in Error calculations), (–)
y	Volume concentration, (–) or %

Greek symbols

α	Selectivity, (–)
Θ	Time lag, s
ϕ	Volumetric flow rate, $cm^3\,s^{-1}$ or $cm^3\,min^{-1}$ (at given p, T)
π	Permeance, $cm^3_{STP}\,cm^{-2}\,min^{-1}\,bar^{-1}$

Subscript/Superscript

0	Instrumental (for the time lag)
Ar	Argon
Atm	Atmospheric
BG	Background
F	Feed
i	Component i, gas species i
Int.St.	Internal standard
j	Component j, gas species j
m	Molar
Mem	Membrane
MS	(inside) Mass Spectrometer
P, Perm	Permeate
Raw	Raw, uncorrected signal
t	Time

nonlinear sorption isotherm, respectively. Complex problems like cluster formation may require different solutions, assuming for instance the simultaneous existence of different diffusion coefficients [22,23]. Despite the simplicity of the time lag method, a problem for highly condensable vapours like water is that sorption of the vapour at the wall of the permeate compartment may lead to a dramatic underestimation of the permeability and an error in the diffusion coefficient [24]. In such cases, gravimetric sorption kinetics studies may provide a better method for the determination of the diffusion coefficient, while the equilibrium sorption yields the solubility.

Most available methods to measure permeability involve single gas or vapour species, which is a strong limitation considering that in many applications the individual gas species influence each other in a mixture. Relatively few papers discuss mixed gas sorption, providing solubility data of the individual gases in a mixture, e.g. [25–27]. Mixed gas permeation measurements are not straightforward because of complications in the analysis itself, and due to interactions between the species in the gas mixture, especially when dealing with polymers with nonlinear sorption behaviour, strong physical aging or slow dilation [9]. Normally, these measurements are carried out in a cross-flow cell configuration by the variable volume method, using gas chromatographic (GC) analysis of the gas composition. This is a relatively slow technique with a sampling time of several minutes per point for normal GC or slightly less than a minute for micro-GC, which may yield steady state permeation data but it does not allow the analysis of transient phenomena in 'fast' materials, and thus the determination of the mixed gas diffusion coefficients. A combination of ^1H and ^{13}C NMR spectroscopy and pulsed-field gradient NMR, studied for this purpose, allowed the determination of the solubility and diffusion coefficients of pure carbon dioxide and its mixtures with other gases [28]. However, this method is not suitable for routine analysis. Chen et al. proposed a rather laborious time lag method for gas-vapour mixtures, where one component was selectively condensed [29]. Instead, on-line mass spectrometry (MS) was proposed as an advanced on-line analytical method for process monitoring and control thanks to its high analysis speed and the possibility to provide real-time information on the process parameters [30]. The fast analysis makes it also suitable to follow Isotopic-Transient Kinetics in chemical reactions [31]. Interestingly, both flat and hollow fibre membranes are proposed as an alternative for the direct capillary inlet to the MS [30], not taking into account the dynamics of the membrane itself in the mass transport. Indeed, membrane inlet mass spectrometry (MIMS) is considered as a special technique, where the high permeability of the membrane should guarantee a quick response and its selectivity should enhance the sensitivity towards specific species, in particular vapours [32] or dissolved gases [33]. Instead of using membranes for the sake of the analysis, Schäfer et al. proposed to follow the mass transport in pervaporation membranes on-line by MS analysis [34]. Similarly, Zhang et al. determined the relative humidity dependence of H_2 and O_2 permeation in ionomer membranes for polymer electrolyte fuel cells [35]. Isotopic-transient permeation experiments under the steady-state pervaporation operation of rubbery polymer membranes allow the determination of concentration-dependent diffusion coefficients of penetrants [36]. Recently, the group of Crespo analysed the transient phenomena related to

the membrane transport by on-line, quantitative monitoring of the organophilic pervaporation [37,38] and gas separation [35,39] processes. In addition, Mass Spectrometric Residual Gas Analyser (MS-RGA) has been used to study permeate under steady state permeation conditions of various Polymers of Intrinsic Microporosity (PIMs) [40–43] or for analysis of solute-membrane interaction in conventional materials via transient permeation [44]. Tremblay et al. previously described a method based on a MS-RGA for the analysis of permeability and diffusivity of pure He, N_2, CO_2 and CH_4 in four different rubbers. However, the much lower CO_2 permeability and CO_2/N_2 selectivity, in for instance polydimethylsiloxane (PDMS), as compared to the literature values raises serious concerns about the accuracy of their method [39].

Here we describe a reliable method to study the transient phenomena during mixed gas membrane permeation and to determine the permeability and diffusion coefficient of the individual components in the mixture. We will discuss the use of MS-RGA for the continuous online analysis of the permeate gas composition, identifying all relevant instrumental and operational parameters and comparing the mixed gas transport data with those obtained with the classical time lag method in a fixed volume setup for pure gases. The technique was developed using two different well-established membrane materials (Pebax® rubbery polymer and Hyflon® glassy perfluoropolymer), and validated with the glassy high performance polymer PIM-EA-TB (Scheme 1). This study illustrates the technique's wide applicability for permeability and diffusivity measurements and the capacity to identify fundamental trends, such as absolute and partial pressure dependence and gas composition dependence of the transport parameters. Finally, analysis of the experimental error will show that the method can be used to calculate the gas diffusion coefficient with a reasonably small error for membranes with a time lag of some ten seconds or higher.

2. Materials and methods

2.1. Materials

Ethanol, absolute AnalaR NORMAPUR® ACS was supplied by VWR Chemicals (Italy). 1-Methoxy-perfluorobutane (HFE 7100) was purchased from 3 M. Hyflon® AD60X was purchased from Solvay-Solexis (Italy) and Pebax® 2533 was kindly provided by Arkema (Italy). All products were used without further purification, unless specified otherwise.

The Tröger's base containing polymer of intrinsic microporosity, PIM-EA-TB, was synthesized as described previously [41] and the membrane was prepared in the form of a dense self-standing film by solvent casting and very slow evaporation of the solvent. Since PIMs are known to undergo strong physical aging [45,46], a film sample aged for more than 6 months following methanol treatment was used for the permeation tests to minimize this performance variable.

2.2. Gases

Pure gases were supplied by Pirossigeno (Italy) at a minimum purity of 99.9995% and by Praxair (Portugal) at a minimum purity of 99.99%. Certified gas mixtures (CO_2/CH_4 with 47.89 mol% CH_4, and $N_2/CO_2/O_2$ with 10.10 mol% CO_2 and 10.02 mol% O_2) were supplied by Sapio (Italy). The purity was ± 0.01 mol% from the certified concentration.

2.2.1. Mass flow controller calibration

Custom-made gas mixtures were prepared in situ by mixing of the pure gases using calibrated EL-Flow electronic mass flow controllers (MFC) (Bronkhorst, STV Portugal). For optimum accuracy, the MFCs were calibrated periodically to check for deviations from the factory standard and to guarantee precise gas dosage. The gas flow rates were determined at ca. 10 different flow rates in the range used for the future measurements. The measurement of the flow rate was performed with a bubble flow meter or with a digital flow meter (ADM2000 Universal Gas Flowmeter, Agilent Technologies), appropriately correcting for atmospheric temperature and pressure.

2.3. Membrane preparation

Hyflon® AD60X membranes were prepared as described previously, from a 5 wt% solution of the polymer, prepared by magnetic stirring of the polymer powder in the solvent HFE 7100 for 24 h at room temperature, normally 23 ± 2 °C [47,48]. The homogenous solution was filtered through a 0.45 μm Teflon PTFE syringe filter and poured into a stainless steel casting ring resting on a glass plate and partially covered with a petri dish to slow down the evaporation. Dense membranes were obtained by solvent evaporation for 72 h at room temperature and the membranes were used as such for the permeation tests. ***Pebax® 2533 membranes*** were prepared according to the procedure reported previously [49], dissolving Pebax® 2533 at a concentration of 10 wt% in ethanol under slight reflux, while magnetically stirring for at least 2 h. The solution was cast into a stainless steel casting ring placed on a Teflon plate and covered with a Petri dish to slow down evaporation. The solution was left for 48 h to allow complete solvent evaporation at room temperature. After this time, self-standing dense membranes were obtained. ***A PIM-EA-TB membrane*** was cast from chloroform, dried in air and then methanol treated to remove residual solvent and to reset the casting history as described previously [41]. The sample was stored for over six months to allow significant initial aging and reach a more stable and time-independent performance [43].

For all membranes, a proportionally larger amount of solution was used to obtain thicker films.

2.4. Experimental set-up and operating conditions

2.4.1. Fixed volume time lag system for pure gases

All gas permeability measurements were performed at 25.0 ± 0.5 °C and at 1 bar, unless specified otherwise, comparing three different instruments, based on either the fixed volume or the variable volume method. The fixed volume-pressure increase instrument, constructed by EESR is an improved version of the instrument described previously [48] and is schematically displayed in Fig. 1. The instrument is equipped with a fixed feed volume of about 2 l and a fixed permeate volume. The permeate volume is expandable from 91.6 cm^3 to 260 cm^3 if it is necessary to reduce the pressure increase rate and to prolong the time available to reach steady state. A set of two membrane pumps and a turbo molecular pump (Pfeiffer), guarantee a high and oil-free vacuum ($< 10^{-3}$ mbar) for effective degassing of the samples. The instrument is provided with eight gas connections and an additional liquid flask for vapour transport measurements. The maximum feed pressure of 2 bar is read with an accuracy of 0.1 mbar; the maximum permeate pressure of 13.3 mbar is read with a resolution of 10^{-4} mbar.

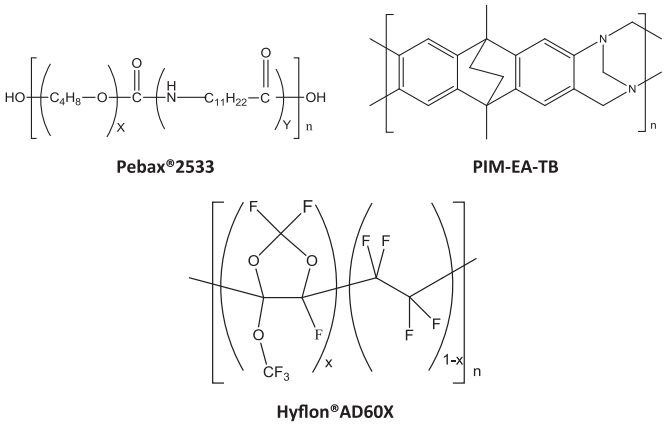

Scheme 1. Chemical structures of the polymers used in the present work.

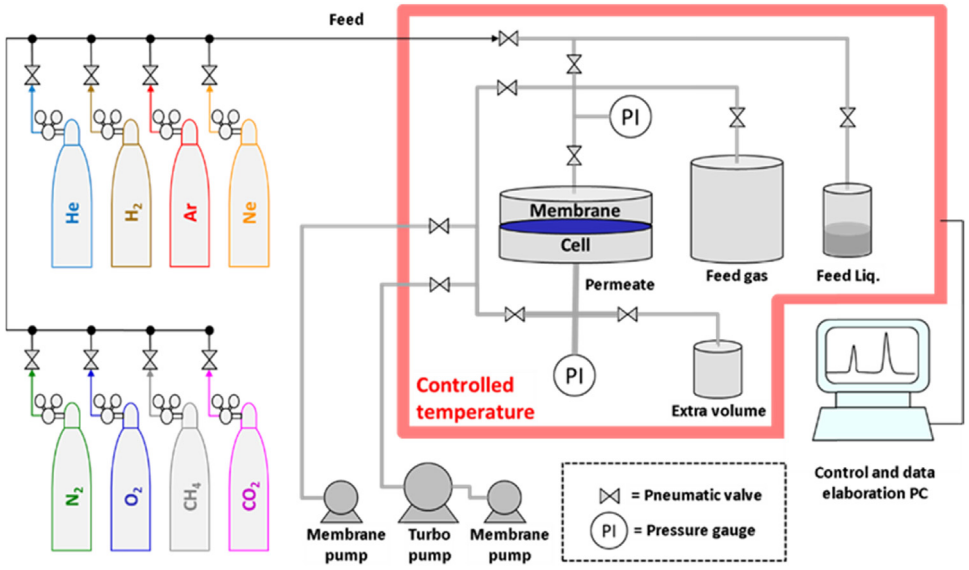

Fig. 1. Scheme of the fixed volume/pressure increase time lag setup.

The 75 mm circular membrane can be fitted with appropriate aluminium masks to reduce the effective test area. Pneumatic valves automatically fill the feed volume at the desired pressure and alternate the gases in subsequent measurements. All valves are computer controlled, guaranteeing extremely short response times. The crucial parts of the setup are placed in a thermostatic chamber to perform measurements at a fixed or a stepwise changing temperature. The feed pressure, permeate pressure and temperature are continuously monitored and exported to a data file for subsequent analysis of the time lag, diffusivity, permeability and gas or vapour solubility.

The measurement is carried out on circular membranes, typically with an effective exposed area of 13.84 cm^2. Smaller samples down to 1.77 cm^2 are prepared by masking with adhesive aluminium foil both for highly permeable membranes, to reduce the effective area, or for

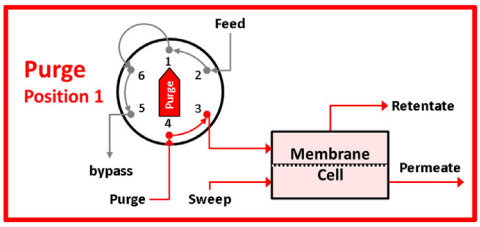

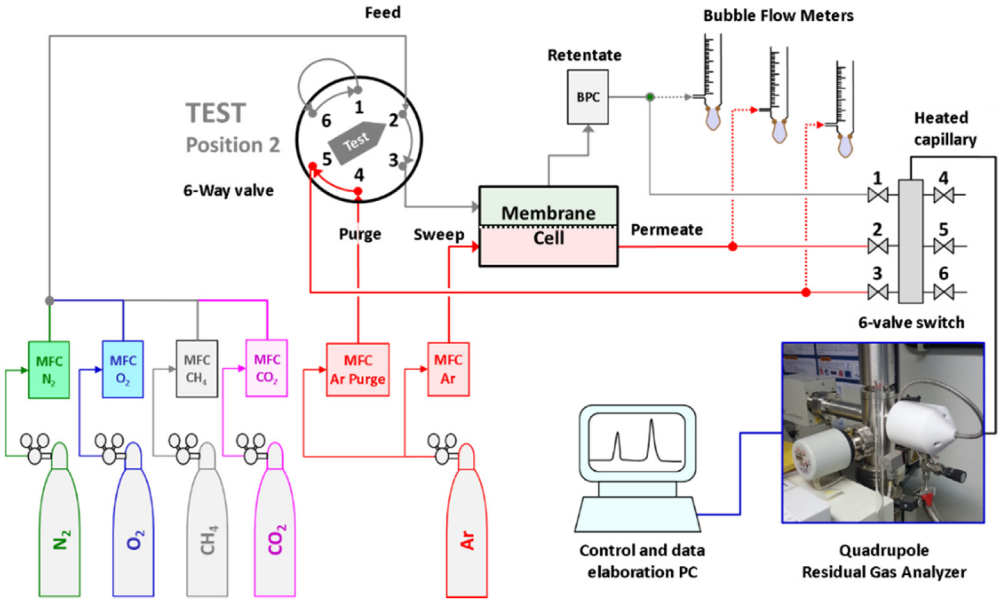

Fig. 2. Scheme of the mixed gas permeation setup in the test mode, with quadrupole gas analyser optimized for operation with a sweeping gas at the permeate side of the membrane. In the purge mode, with the 6-way valve in the 1-position (insert), argon purge gas flows from connection 3–4 through the feed side of the membrane cell and the feed flow is bypassed via connections 2-1-6-5.

fragile samples to prevent cracking under the sealing ring. At the beginning of each test, the membrane is degassed under high vacuum inside the permeation cell for sufficient time to remove all absorbed species (usually > 1 h). Evacuation is stopped if the baseline drift is significantly below the expected steady state pressure increase rate with the relevant gases [48]. After every run, the membrane is evacuated for a period of at least 10 times the time lag in order to completely remove the previous penetrant from the membrane. The entire permeation curve is determined, including the initial transient, to allow the determination of the diffusion coefficients of the penetrants by the time lag method (Annexure A), and the determination of the permeability coefficient from the steady state pressure increase rate.

2.4.2. Variable volume system using mass spectrometry for pure and mixed gases with the permeate under sweeping gas conditions

The instrumental setup for the mixed gas permeation measurements with sweeping gas is displayed in Fig. 2. The key element of the system is a mass spectrometric residual gas analyser (Hiden Analytical, HPR-20 QIC Benchtop residual gas analysis system) equipped with a quadrupole mass filter (max. 200 AMU) and a heated sampling capillary with a typical flow rate of ca. 12 cm^3_{STP} min^{-1} argon at atmospheric sampling pressure. The electron ionization energy is 70 eV and the gases at low partial pressures are generally detected with the Secondary Electron Multiplier (SEM) ion detector. The Faraday detector is used for gases at higher partial pressures.

The permeation setup consists of a custom made constant pressure/variable volume system, equipped with a modified Millipore permeation cell (diameter 47 mm). The feed and retentate connections at the upstream side, and the sweep and permeate connections at the downstream side, are positioned in such a way to promote a spiral-like flow profile and to minimize tangent regions or polarization phenomena inside the cell. The cell is fed with the pure and mixed gases by means of EL-FLOW electronic mass flow controllers for each gas (Bronkhorst), and the pressure is controlled with an EL-PRESS electronic back pressure controller (Bronkhorst) in the retentate line. Two independent mass flow controllers provide argon continuously to the permeate side of the cell as a sweeping gas, and periodically to the feed side of the cell when it is in purge mode between two measurements. The measurement cell and part of the connections are located in a thermostated chamber to guarantee operation at controlled temperature. The MS-RGA is connected to the permeate via a heated capillary and excess of the permeate/sweeping gas freely flows via a T-connection to the atmosphere. The flow rates are frequently checked by two glass bubble flow meters in the retentate line and in the permeate line, which are also used for the periodic calibration of the mass flow controllers. The actual temperature and pressure are recorded to convert the measured bubble flow rates to standard temperature and pressure conditions (STP, 273.15 K and 1.01325 bar).

The mixed gas permeation experiments were carried out at a feed flow rate of 100–200 cm^3_{STP} min^{-1} and a controlled feed pressure of 0–5 bar(g). The argon sweeping gas was normally set at a flow rate of 30 cm^3_{STP} min^{-1}. The permeate composition was determined via Mass Spectrometric analysis of the permeate/sweep stream, using the ^{36}Ar signal as the internal standard. Since too high humidity is known to affect the other signals and reduce the sensitivity to detect other gases by chemical reactions taking place at the filament [50], only high purity dry argon is used. Highly permeable samples were masked to limit the total permeate flow rate and to keep the stage cut close to or below 1%.

Before each analysis, the membrane was flushed for at least 1 h at both sides with two independent argon streams until the MS signal was sufficiently stable, and this signal was taken as the background. Subsequently, the argon flux at the feed side was instantaneously replaced by the pure gas or the gas mixture at atmospheric pressure (absolute pressure 1 bar(a)) via the 6-way valve, and the gas concentrations in the permeate were followed as a function of time for a sufficiently long time to reach steady state. Thus, the time lag (Section 2.4.1 and Annexure A) and the permeation rate were determined after reaching steady state, and no special approximations or procedures were needed, like when only part of the transient curve is used to calculate the transport parameters [23,51]. If desired, in a second experiment, the feed pressure was stepwise changed from 1 to 5 bar(g) and back, with sufficiently long time intervals to reach steady state permeation in each step.

2.4.3. Variable volume system using mass spectrometry for pure and mixed gases with the permeate under vacuum conditions

The setup for performing pure and mixed gases separation experiments with mass-spectrometric analysis of the permeate under vacuum conditions is displayed in Fig. 3. The main difference compared to the sweeping gas setup is the direct connection of its permeate side with the mass spectrometer via a restriction. The permeate side is kept at low pressure using a dry and oil-free diaphragm vacuum pump (Pfeiffer vacuum, MVP 015) and a low constant argon flux is used as an internal

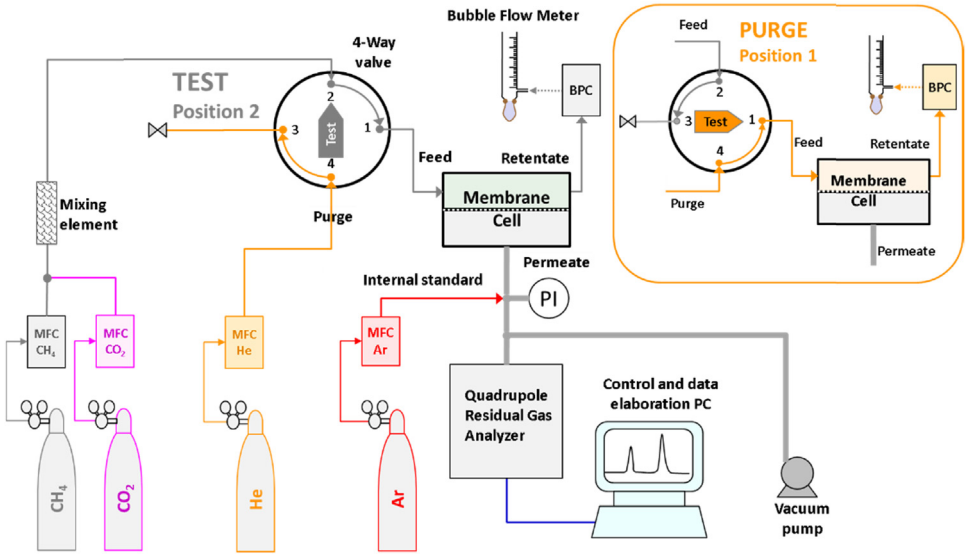

Fig. 3. Scheme of the mixed gas permeation setup with quadrupole MS-RGA optimized for vacuum operation at the permeate side of the membrane in test mode and during purge with helium (Insert).

standard (1 cm^3_{STP} min^{-1}). The unit comprises a membrane permeation cell and mass flow controllers (EL-FLOW electronic mass flow controllers, Bronkhorst) for each gas, and the pressure is controlled with an EL-PRESS electronic back pressure controller (Bronkhorst). The permeate composition is monitored on-line with a frequency of approximately one second, using a mass spectrometer connected directly to the permeate. The mass spectrometer (Prisma Plus QMG 220 M2, Pfeiffer Vacuum) was used in an axial beam ion source, emission current 1 mA, electron energy 70 eV, single quadrupole, secondary electron multiplier SEM detection. In each permeation experiment with a defined feed gas/mixture of gases, the following operating parameters were controlled and measured: the gas feed pressure gas was maintained at 1.05 bar(a), the total flow rate of the inlet feed stream was 50 cm^3 min^{-1} of the gas/mixture of gases and a flow rate of 1 cm^3 min^{-1} of ^{40}Ar (internal standard) was fed directly to the permeate. The temperature of the system was kept at 17 ± 1 °C.

Before each permeation experiment, the feed side of the membrane cell was purged with helium in order to clean the membrane and the system from other gases (*purge mode, position 1* in Fig. 3). Following the concentrations of all gases under study in the permeate through the MS, and ensuring that all of them are at the noise level, the gas under study is introduced into the feed side, using a 4-way valve (*test mode, position 2* in Fig. 3) and the permeation of each gas/mixture of gases through the membrane is monitored over the time in terms of volume fraction concentration and partial pressure in the permeate compartment.

2.5. Mass spectrometric permeability measurements

2.5.1. Analysis of the gas composition

The mass spectrometer gives a characteristic spectrum for compounds and their fragments after ionization, according to their specific mass to charge ratio (m/z) and intensity. For the light gases used in the present work, the molecular peak or one of the fragments is normally used, and occasionally a characteristic isotope. In the absence of hydrocarbons, nitrogen is detected here at $m/z = 14$ amu (AMU), to avoid overlap of N_2 with the CO fragments from CO_2 at $m/z = 28$ AMU in CO_2/N_2 mixtures; methane is detected at $m/z = 15$ AMU (as CH_3) to avoid overlap of the molecular CH_4 peak with the O fragment from CO_2 at $m/z = 16$ AMU in the case of CO_2/CH_4 mixtures. All sensitivity ratios are previously calibrated against the weaker ^{36}Ar isotope at $m/z = 36$ AMU (ca. 0.3% abundancy) for the sweeping gas system, and ^{40}Ar $m/z =$ 40 AMU for the vacuum system, both used as internal standards.

In the first step, the background signal, I_{BG}, is measured while purging the membrane with argon at the feed and permeate side. This signal is subtracted from the raw data signal in all experiments:

$$I_i = I_{raw,i} - I_{BG,i} \tag{1}$$

All measurements in the unit working under sweeping gas conditions were recorded with the MASsoft software package supplied with the mass spectrometer (Hiden), while the FlowPlot software (Bronkhorst) supplied with the pressure and mass flow controllers registered the pressure and gas flow rates. The raw partial pressure data were elaborated by a macro in MS Excel after synchronization of the time scales of the two sources of data. Multiplication of the background-corrected signal with the relative sensitivity, RS_i, yields the partial pressure in the gas analyser, $p_{MS,i}$,

$$p_{MS,i} = I_i/RS_i \tag{2}$$

For the sweeping gas system with an open connection of the permeate side to the air, normalization for the atmospheric pressure yields the partial pressure in the permeate/sweep stream:

$$p_{P,i} = p_{Atm} \cdot \frac{p_{MS,i}}{\sum_i p_{MS,i}} \tag{3}$$

The measurements in the unit working under vacuum conditions were recorded using QUADERA software provided with the mass spectrometer and the pressure and flow rates were acquired with FlowPlot software provided with the pressure and flow controllers. The output of the mass spectrometer is the electrical signal, I_i (A), used to calculate the volume concentration of each gas y_i (vol%), and the partial pressure of each gas p_i (mbar) from the total pressure in the permeate, p_{total} (mbar):

$$y_i = y_{Ar}/RS_i \cdot \frac{I_{Ar}}{I_i} \tag{4}$$

$$p_i = y_i \cdot p_{total} \tag{5}$$

2.5.2. Determination of the permeability coefficient

When using sweeping gas conditions, the permeation rate of each species follows directly from the known sweep flow rate, Q_{Ar}, and the ratio of partial pressures of the gas of interest (Eq. (3)) and of argon, p_{Ar}:

$$Q_{P,i} = Q_{Ar} \cdot \frac{p_{P,i}}{p_{Ar}} \tag{6}$$

This yields the permeability coefficient, P_i, and permeance, Π_i, for each component:

$$P_i = \frac{Q_{P,i} \cdot l}{(p_{F,i} - p_{P,i})A} \tag{7}$$

$$\Pi_i = \frac{Q_{P,i}}{(p_{F,i} - p_{P,i})A} \tag{8}$$

where l is the membrane thickness, A is the membrane area and $p_{P,i}$ is the partial pressure of gas i in the feed:

$$p_{F,i} = x_i \cdot p_F \tag{9}$$

where x_i is the mole fraction of gas i in the feed and p_F is the feed pressure. The mixed gas selectivity is calculated as the ratio of the permeability coefficients or permeances:

$$\alpha_{i/j} = \frac{P_i}{P_j} = \frac{\Pi_i}{\Pi_j} \tag{10}$$

An important parameter is the stage cut, defined as the fraction of each component in the feed gas which permeates the membrane, and it is given by:

$$Stage\ \ cut_i = \frac{Q_{P,i}}{Q_{F,i}} \times 100\% = \frac{Q_{P,i}}{x_i \cdot Q_F} \times 100\% \tag{11}$$

where Q_F is the total feed flow rate. This value should be low to guarantee that no significant polarization phenomena occur.

The data evaluation procedure is similar for the gas permeation under vacuum conditions. In this case, the volumetric flows of the gas (es) under study and the argon in the downstream circuit of the permeation cell, respectively Q_i and Q_{Ar} (cm^3_{STP} min^{-1}) and the partial pressure of each gas, p_i and p_{Ar} (mbar), are related to each other according to equation:

$$\frac{Q_i}{Q_{Ar}} = \frac{p_i}{p_{Ar}} \tag{12}$$

The flux of each gas in the permeate, J_i, (cm^3_{STP} cm^{-2} min^{-1}) is the ratio of the flow rate of the gas through the membrane and the membrane area (cm^2), and can be written as:

$$J_i = \frac{Q_{Ar}}{A} \cdot \frac{p_i}{p_{Ar}} \tag{13}$$

The permeability coefficient and selectivity are the same as in Eqs. (7) and (10).

3. Results and discussion

3.1. Membrane preparation

The thicknesses of the membranes prepared in this work are listed in SI Table 1. Both for the Pebax® and for the Hyflon® membranes, there is a slight variation in the properties depending on the casting procedure and the membrane thickness. Pebax® is a semi-crystalline rubbery polymer with microphase separation of the polyether and polyamide domains, and the evaporation rate affects to some degree the micro-domain size and the crystallinity. On the other hand, Hyflon® is known to retain residual solvent upon evaporation [47,48], and since the evaporation speed is thickness dependent, this will influence gas transport properties. Both effects may thus lead to variation of the transport properties and therefore more samples were prepared, and only the ones with the most constant properties were selected for further evaluation. The PIM-EA-TB sample was solvent-cast and then methanol treated to reset the thermomechanical history, and subsequently aged for over six months to reach a stable performance. Aging took place under atmospheric conditions without control of humidity, air exposure or any other special treatment.

3.2. Pure gas permeation in the fixed volume time lag system

For all measurements, the results of the fixed volume time lag setup were used as a reference. For this purpose, two well-defined and reproducible samples were tested, namely the rubbery Pebax® 2533 and the glassy Hyflon® AD60X. Fig. 4A and C show the permeability and ideal selectivity for several gas pairs in five Pebax® 2533 samples with different thicknesses and, Fig. 4B and D show the same data for four

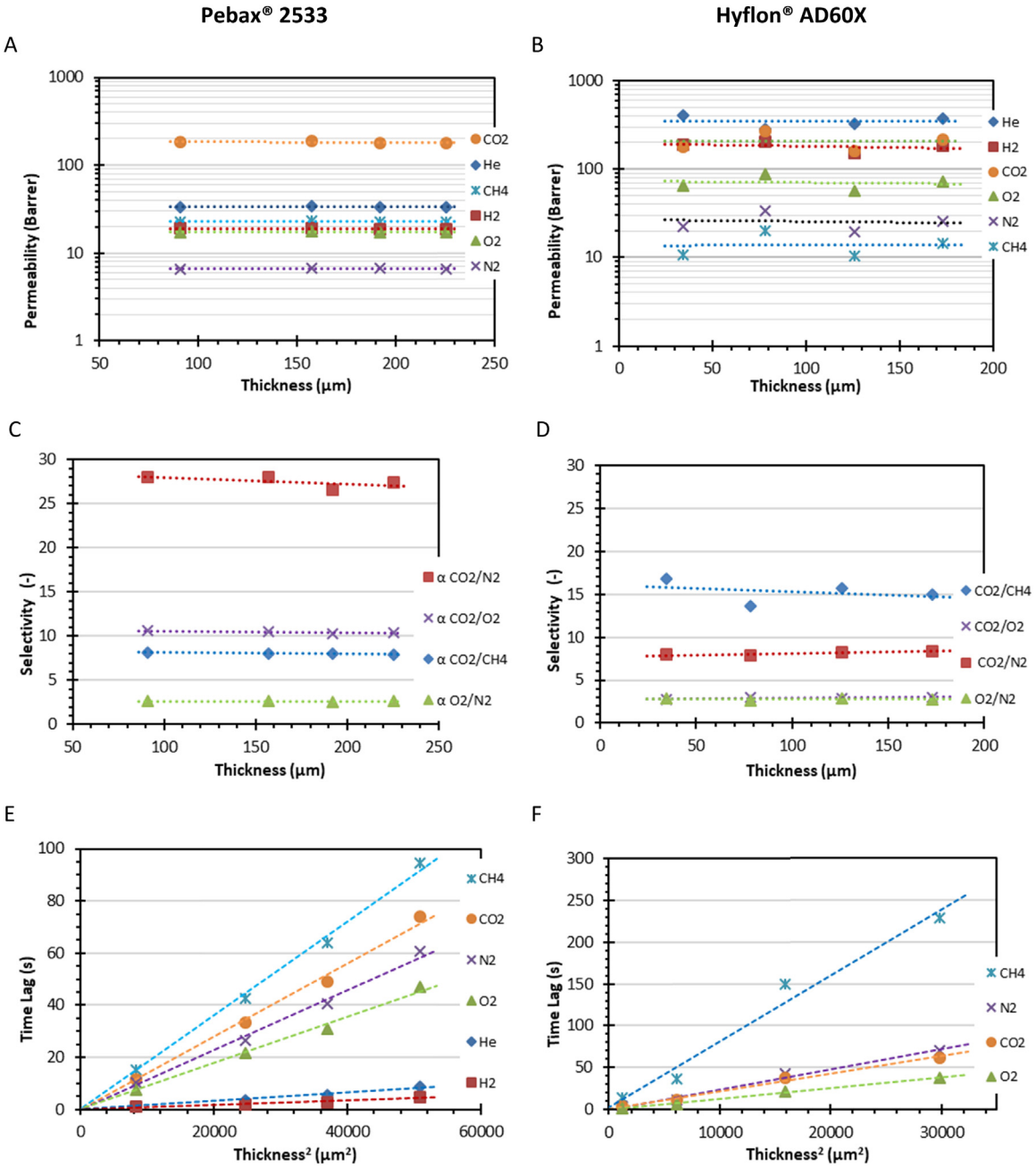

Fig. 4. Thickness dependence of permeability (A,B) for Pebax® 2533 (left) and Hyflon® AD60X (right) with their ideal selectivity (C, D) for selected gas pairs. Determination of the diffusion coefficient for membranes with different thicknesses according to Eq. (14), $D = l^2/6\Theta$ (E, F).

samples of Hyflon® AD60X. Beyond some random scatter in the data due to experimental error, there is no significant impact of the thickness on the permeability and selectivity. For this system, the diffusion coefficient is determined by the well-known time lag procedure based on the penetration theory [17,18]. A detailed description of the calculation procedure is given in Annexure A. Under normal conditions, the time lag, Θ, is proportional to the square of the membrane thickness, l, and inversely proportional to the diffusion coefficient, as in the simple equation:

$$\Theta = \frac{l^2}{6D} \tag{14}$$

Fig. 4E and F show the dependence of the time lag on the square of the thickness for both polymers, confirming that for all tested gases the time lag follows Eq. (14) with only few seconds of experimental error (See Annexure C). This means that the diffusion coefficient is essentially thickness-independent. For a microphase separated semi-crystalline block copolymers such as Pebax® 2533 this is not obvious because the microdomain formation [49], and indirectly the transport properties, may depend on the evaporation rate and thus on the thickness of the cast film. In any case, the present tests confirm that these four samples are suitable standards for the evaluation of the mixed gas transport properties. The same is valid for the Hyflon® samples, although these samples show slightly more scattering in both the permeability and the time lag values, probably because their transport properties are known to be dependent on traces of trapped residual solvent in the polymer [47,48]. For this reason, the data for Hyflon® are suitable for validation of the method, but they are not accurate enough to be used as a reference material for determination of the instrumental time lag (Section 3.3.3). Due to their glassy nature, the Hyflon® samples show a much stronger size selectivity than Pebax®, resulting in a higher helium permeability than the CO_2 permeability and in a much longer time lag for the relatively bulky CH_4 than for the smaller molecules.

As an additional check, Fig. 5 shows the response of the instrument for an aluminium foil sample with a single pinhole. In spite of the very tiny hole, the pressure increase rate of this film is extremely fast, because pore flow is orders of magnitude faster than diffusion through dense films. All six tested gases show a very short delay of less than 0.1 s (inset) in the pressure increase curve, and the pressure of the first point is insignificant compared to the increase rate during the experiment. This confirms that the instrumental time lag for this machine is negligible compared to the time lags observed in the Pebax® samples in Fig. 4E and F. The pressure increase rate and thus the apparent permeance of the pinhole show the typical Knudsen behaviour, for which the permeance is inversely proportional to the square root of the molar mass, M_i, of the permeating species and the linear regression curve passes through the origin:

$$P_i \propto \frac{1}{\sqrt{M_i}} \tag{15}$$

3.3. Gas permeation in the variable volume mixed gas systems

3.3.1. Notes on the instrumental time lag in the mixed gas system

In contrast to the extremely fast pressure measurement described above, the response of most other gas analysers depends not only on the time lag of the membrane itself, but there may be an additional instrumental time lag related to setup, representing the total delay of the permeating gas in the system before reaching the analyser. If we assume both contributions independent from each other, then the measured time lag is given by:

$$\Theta_i = \Theta_0 + \Theta_{Mem,i} \tag{16}$$

where Θ_0 is the instrumental time lag and $\Theta_{Mem,i}$ is the time lag induced by the diffusive transport across the membrane itself for each gas species i. For the constant pressure/variable volume systems in the present work, Θ_0 reflects the total residence time of the permeating gas in the system, and is indeed not negligible. Substituting Eq. (14) in Eq. (16) yields:

$$\Theta_i = \Theta_0 + \frac{l^2}{6D_i} \tag{17}$$

Thus, for a set of membranes with different thicknesses, a plot of Θ versus l^2 should yield a straight line with slope $1/6D$, intersecting the vertical axis at the value Θ_0. Once the value of Θ_0 is known, the diffusion coefficient can be determined for any membrane by a single measurement, after subtraction of the instrumental time lag from the overall time lag:

$$D_i = \frac{l^2}{6(\Theta_i - \Theta_0)} \tag{18}$$

The residence time of the gas in the analyser and in all tubing of both mixed gas setups (Figs. 2 and 3) contributes to the overall time lag. The individual sections contributing to the residence time are highlighted in Fig. 6. Only the sections directly after the four- or six-way

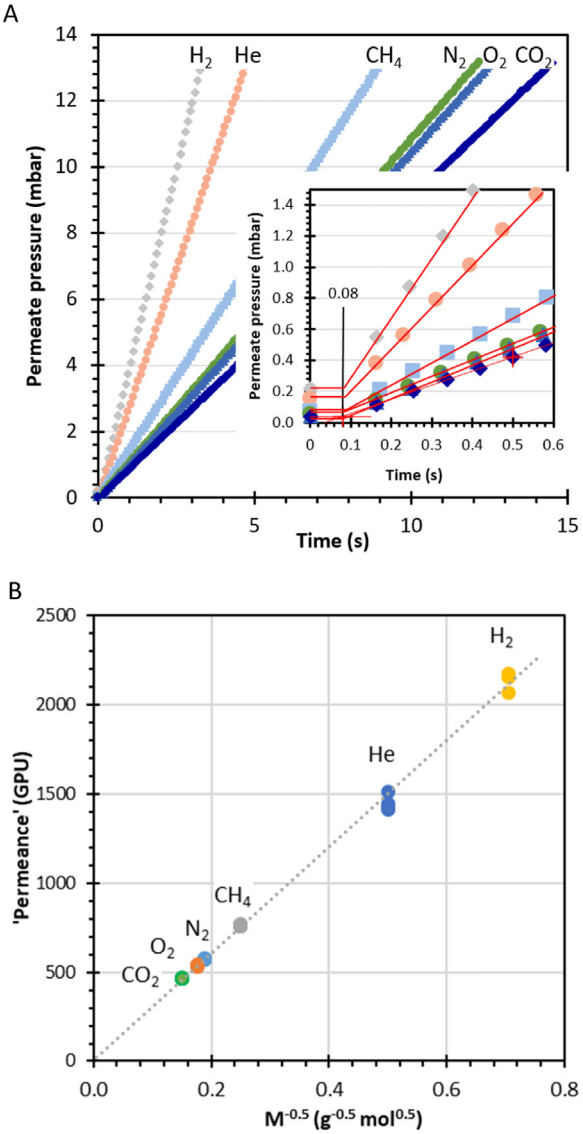

Fig. 5. (A) Determination of the instrumental time lag by an aluminium foil sample with a pinhole defect. (B) Evidence of Knudsen flux in a plot of apparent permeance versus $M^{-0.5}$ at different pressures according to Eq. (15). The apparent permeance of different gases calculated on the basis on a hypothetical active area of 2.14 cm^2.

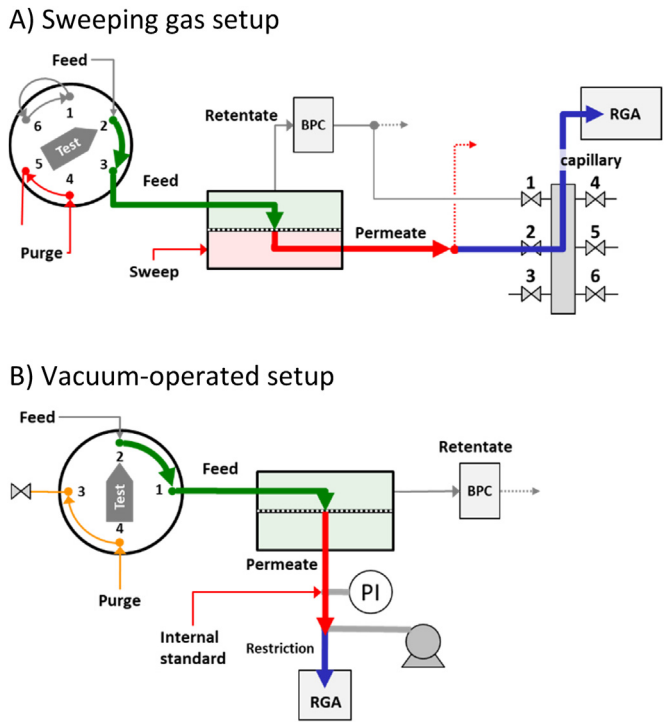

Fig. 6. Scheme showing for both setups the contributions of the flowing gas to the total time lag of the system just after switching from purge to test mode. The feed flow (thick green arrows), permeate/sweep flow (thick red arrows) and flow through the injection port into the analyser (thick blue arrows) each contribute to the instrumental time lag given by Eq. (19). Note the fundamental difference between the sweep gas setup with minimum volume lines in the permeate and analysis section, and the vacuum operated setup with voluminous vacuum connections but with low pressure.

valve are relevant for Θ_0, because the feed stream is already flowing before switching this valve from the purge position to the test position. To optimize the method, each part of the system should have a minimum residence time, and thus thin tubes, so that Θ_0 remains small. On the other hand, the pressure drop in the lines should be low too, which prohibits the use of very thin tubes. For the given system, 1/8″ tubes offer the best compromise between small volume and low pressure drop (See Annexure B). Under the operation conditions generally used, namely a sweep flow rate from 30 $cm^3\ min^{-1}$ up to 50 $cm^3\ min^{-1}$ and a feed flow rate of ca. 200 $cm^3\ min^{-1}$, the flow regime is laminar. This means that the transient related to the gas permeation through the membrane is further widened in the tubes. However, the time lag can still be determined by the tangent method as for the pure gas permeation in the fixed volume setup.

For our systems, we can define instrumental time lag as the sum of the contributions of the feed flow reaching the membrane surface, the downstream flow (permeate plus sweep, if used) reaching the inlet of the mass spectrometer, and the sampled gas flow reaching the analyser across the capillary or the restriction:

$$\Theta_0 = \frac{V_{Feed}}{\phi_{Feed}} + \frac{V_{Downstream}}{\phi_{Downstream}} + \frac{V_{Inlet}}{\phi_{Inlet}} \tag{19}$$

where V_{Feed}, $V_{Downstream}$, and V_{Inlet} are the volume of the feed side, the volume of the permeate side until the sampling point, and the volume of the injection line, respectively. Note that these volumes are obviously constant, and the term '*variable volume method*', used for this system, refers to the fact that the permeate gas flows away from the system. The terms ϕ_{Feed}, $\phi_{Downstream}$, and ϕ_{Inlet} indicate the respective total volumetric flow rates in that part of the setup at given temperature and pressure:

$$\phi = Q \cdot \frac{p_0}{p} \cdot \frac{T}{T_0} \tag{20}$$

For the downstream side in the sweeping gas setup:

$$\phi_{Downstream} = \phi_{Perm} + \phi_{Sweep} \tag{21}$$

where ϕ_{Perm} and ϕ_{Sweep} are the flow rates of the permeating gas and of the sweeping gas, respectively. For the vacuum setup:

$$\phi_{Downstream} = \phi_{Perm} + \phi_{Int.std.} \tag{22}$$

where $\phi_{Int.std.}$ is the flow rate of the internal standard. With the assumption that all terms are independent, for a membrane with a given thickness, the total time lag becomes:

$$\Theta_i = \Theta_0 + \Theta_{Mem,i} = \frac{V_{Feed}}{\phi_{Feed}} + \frac{V_{Downstream}}{\phi_{Downstream}} + \frac{V_{Inlet}}{\phi_{Inlet}} + \frac{l^2}{6D_i} \tag{23}$$

In the case of a barrier film with pinhole defect, the membrane time lag becomes negligible and $\Theta = \Theta_0$. Thus, Eq. (23) offers two independent ways to determine the instrumental time lag, directly for porous membranes without time lag, or via extrapolation of a set of membranes with different thicknesses via:

$$\Theta_0 = \lim_{l \to 0}(\Theta_i) \tag{24}$$

In the sweeping gas system, the value of V_{Inlet} is fixed for the instrument and that of ϕ_{Inlet} is dictated by the capillary used, the type of gas, and the pressure at the permeate side (atmospheric pressure in the current setup). If $\phi_{Perm} \ll \phi_{Sweep}$, then the gas flowing at the downstream side is nearly pure Argon and ϕ_{Inlet} becomes independent of the permeating gas. Theoretically, ϕ_{Inlet} depends also on the atmospheric pressure, which defines the pressure drop over the capillary, but since atmospheric pressure is constant within a few percent, this is believed to cause negligible variation in the overall time lag. The values of V_{Feed} and $V_{Downstream}$ depend on the membrane size, valves and various connections in the experimental setup. If the stage cut is negligible, then for a series of experiments with different ϕ_{Feed} and ϕ_{Sweep}, V_{Feed} can be determined experimentally from the slope of the curve of Θ_i versus $1/\phi_{Feed}$, and if $\phi_{Perm} \ll \phi_{Sweep}$, then $V_{Downstream}$ can be calculated from the slope of the curve of Θ_i versus $1/\phi_{Sweep}$. Alternatively, the different parameters can be solved simultaneously by a least squares fitting procedure (Section 3.4).

In the vacuum system, $V_{Downstream}$ is fixed and should be determined measuring the volume of the tubing. On the other hand, $\phi_{Downstream}$ depends on the permeate pressure and on the pumping speed of the vacuum pump, as well as the flow rate of the internal standard, which must all be kept as constant as possible. Both MS setups have their advantages and disadvantages. Watson and Baron argue that the low-pressure vacuum measurement device is preferable because it avoids interference of the sweeping gas with the permeation process [24]. On the other hand, operation at room temperature with an excess of sweeping gas allows a more stable analysis because the virtually constant composition (> 99% argon) guarantees a constant gas sampling rate through the heated capillary. An advantage of the constant argon flow is also that it can be used as an internal standard.

3.3.2. Sensitivity factor calibration

The relative sensitivities of the different gases specified by the instrument supplier or tabulated in the literature are not universal enough to be used as a standard for high precision analysis [52] and therefore both mass spectrometric instruments were periodically calibrated for the relevant gases. In the present work, full calibration was performed by mixing each gas of interest with argon in the same concentration range expected during the permeability measurements [53]. The relative sensitivity was then determined at different gas ratios to check that it is independent of the composition of the mixture, as it should ideally be. Therefore, the gas mixture was fed into the MS and the relative sensitivity was determined from the ratio of the

background-corrected signals and the ratio of the gas flow rate, Q_i, and the argon flow rate, Q_{Ar}:

$$RS = \frac{I_i}{I_{Ar}} \cdot \frac{Q_{Ar}}{Q_i} \tag{25}$$

This procedure was repeated for each gas or gas mixture of interest, using the membrane cell with a perforated aluminium disc as a mixing element. It gives a better quantitative calibration of the partial pressures then the variable leak method used by Tremblay et al. [39] for a single gas, followed by correction of the ionization for different gases.

The instrument with sweeping gas was calibrated against the concentration of ^{36}Ar, which is with 0.3% natural abundance small enough to be then in the same range as the permeating gases. The instrument operating under vacuum was calibrated against the ^{40}Ar signal, because operating at much lower pressure this signal remains small enough to use the SEM ion detector for all gases. The relative sensitivity factor of each gas against argon is determined to convert the characteristic intensity of each gas present at the permeate compartment ($^{44}CO_2$, $^{15}CH_4$, ^{4}He, ^{40}Ar) in its corresponding concentration (vol%) or partial pressure (mbar). A method of calibration was set using the software Quadera to obtain the calibration factor of each gas in relation to the Argon internal standard. To perform this calibration, the permeate side is evacuated for 3 h to ensure that it is clean and free from traces of gases. After this time, the permeate compartment is fed using the mass flow controllers with the internal standard gas (Argon) at 1 $cm^3\ min^{-3}$ and the gas to be studied with a flow rate of 50 $cm^3\ min^{-1}$, which allows to calculate of the volume concentration of each gas. Having the volume concentration of each gas, Quadera software generates the corresponding sensitivity factor of the gas under study in relation to the internal standard gas. The resulting values of the relative sensitivities in relation to argon for both methods are listed in Table 1. The values of ionization factor correction given by the supplier or given in the literature are typically represented in relation to nitrogen [39]. Recalculated values are given in Table 1 as well. Although, the ionization of different gases under specific experimental conditions (ionization current and ionization energy) should in principle be very reproducible, and although the relative sensitivities are tabulated by the various producers, the different instruments and operation conditions introduce too large deviations to use these values for the calculation of the gas concentrations in the permeation experiments. Lieszkovszky et al. found that in different partial pressure analysers (PPA) the response of a trace gas in argon and that of an argon trace in that same gas may depend differently on the partial pressures of each gas [52]. This confirms that calculations cannot rely on tabulated sensitivity factors, and that calibration must necessarily be performed for each experiment in a specific way that most closely resembles the analysis conditions.

Table 1
Typical relative sensitivity factors for different gases and their selected fragments obtained experimentally in this work and calibrated with reference to argon.

Gas	Signal	Relative sensitivity			
		Sweeping gas setup[a]	Vacuum setup[a]	Reference values[b]	Reference values[c]
Ar	^{40}Ar	n.d.	**1.00**	1.2	n.d.
	^{36}Ar	**1.00**	n.d.	n.a.	**1.00**
CO_2	$^{44}CO_2$	266.2	0.59	1.4	198
	^{28}CO	n.d.	0.01	122.8	22.5
O_2	$^{32}O_2$	202.8	n.d.	0.86	321
N_2	$^{28}N_2$	n.d.	n.d.	**1.00**	277
	^{14}N	29.7	n.d.	13.9	19.9
CH_4	$^{15}CH_3$	254.2	1.02	1.88	173
He	^{4}He	n.d.	0.87	0.14	1980

[a] Experimentally determined under normal operating conditions. Values need periodic calibration.

[b] From MASsoft 7 library and Application note 282: Relative Sensitivity Measurements of Gases, Hiden Analytical.

[c] From MASsoft 7 library and Application note 282: Relative Sensitivity Measurements of Gases, Hiden Analytical. Values normalized for ^{36}Ar.

3.3.3. Instrumental and membrane time lag determination

A typical measurement curve for the sweeping gas setup (Fig. 2) is displayed in Fig. 7A. In contrast to the fixed volume setup, where the pressure in the permeate volume represents the total amount of permeated gas, the standard signal of the MS is the concentration of the gases in the permeate, which must be converted into the gas flow rate for each component, according to Eq. (6). Integration of this signal yields the cumulative permeated gas volume [54]. Thus, the total permeate volume, $V_{P,i}$, is obtained by integration of the flow rate:

$$V_{P,i} = \int_{t=0}^{\tau} Q_{P,i}\, dt \tag{26}$$

or for discrete measurement intervals:

$$V_{P,i} = \sum_{t=0}^{\tau} \left(\frac{Q_{P,i,t} + Q_{P,i,t+\Delta t}}{2} \right) \cdot \Delta t \tag{27}$$

An example of this procedure is given in Fig. 7B.

The unique feature of this procedure is that the online analysis of the gas composition by the MS signal is fast enough to allow simultaneous analysis of all components as a function of time, in contrast to analysis by gas chromatography, which may take up to several minutes

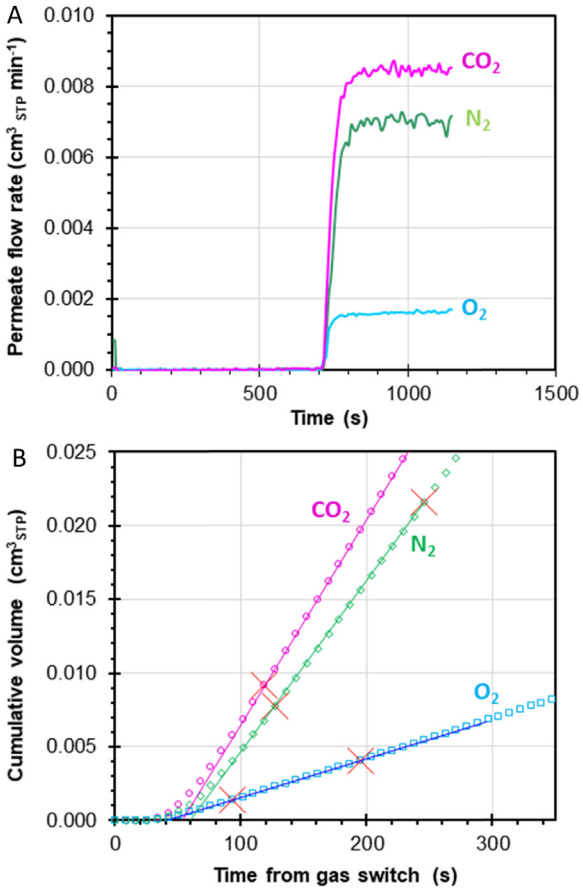

Fig. 7. A) Example of the N_2, CO_2 and O_2 permeate flow rates as calculated by Eq. (6) from the start of the experiment, including 10 min for determination of the baseline. B) Corresponding cumulative permeate volumes after switching from purge mode to test mode, as determined by Eq. (27), allowing for the simultaneous determination of all components in the gas mixture. Gas mixture: $N_2/CO_2/O_2$ 80/10/10 vol%, Membrane: 126 µm Hyflon® AD60X dense film. Red crosses indicate the fitting interval of the tangent.

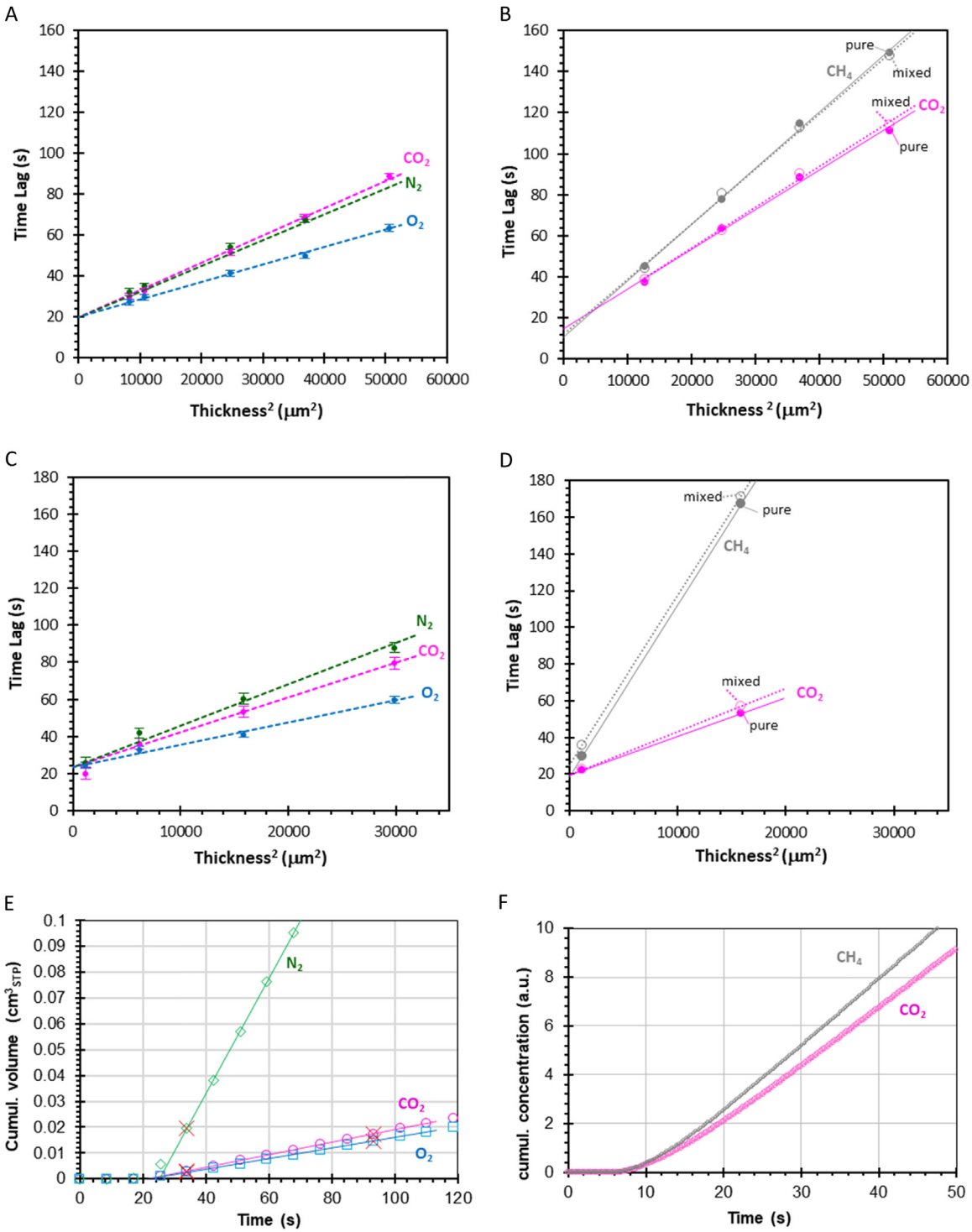

Fig. 8. Determination of the instrumental time lag for membranes with different thicknesses according to the equation $\Theta_i = \Theta_0 + l^2/6D_i$ for Pebax® 2533 (A) and Hyflon® AD60X (C) in the sweeping gas setup at a sweep flow rate of 30 cm^3 min^{-1} and with gas mixture $N_2/O_2/CO_2$ 80/10/10 vol%. Dashed lines describe the fit according to the procedure in Annexure C. Analogous results in the vacuum permeate setup (B, D) with pure CO_2 and CH_4 and in the 50/50 vol% CH_4/CO_2 mixture. Lines correspond to a linear least squares fit of the individual points. Comparison with the instrumental time lag determined by an aluminium foil sample with a pinhole defect in the sweeping gas setup (E) and the vacuum setup (F), respectively. In all cases the error bars are close to the size of the symbol.

for each single point.

After integration of the volumetric flow rate, the procedure for the determination of the overall time lag is then fully equivalent to that described for the pure gases. The instrumental time lag was determined by measuring the time lag for a number of Pebax® 2533 and Hyflon® AD60X membranes with different thicknesses. Fitting of the experimental data with Eq. (17) in a plot of the time lag as a function l^2 yields Θ_0 as the intercept with the vertical axis, and $1/6D_i$ as the slope of the curve (Fig. 8). The Pebax® data extrapolate to an instrumental time lag of ca. 21 s in the sweeping gas unit for mixed gas, and to a value of ca. 13 s in the vacuum gas unit, for both pure and mixed gas (50 vol% CO_2 in CH_4). The scatter is somewhat large for the Hyflon® sample set, and the intercept with the vertical axis yields too large differences with the different gases to be sufficiently reliable as the instrumental time lag.

Table 2
Gas diffusion coefficients (10^{-12} m^2 s^{-1}) in Pebax® 2533 and Hyflon® AD60X determined by different methods.

		Fixed volume setup[a]	Mixed gas variable volume setup		
			Sweep mode[b]	Vacuum mode[c]	
Polymer	Gas	Pure gases	(N_2/CO_2/O_2 80/10/10 vol%) Mixed gases	Pure gases	(50 vol% CO_2 in CH_4) Mixed gases
Pebax® 2533	N_2	145 ± 3.9	138.0 ± 4.6	n.d.	n.d.
	O_2	188 ± 4.5	196.8 ± 15.6	n.d.	n.d.
	CO_2	119 ± 3.0	121.8 ± 6.4	85.8 ± 3.5 (115.6)[d]	83 ± 2.4 (112.4)[d]
	CH_4	92.5 ± 2.0	n.d.	60.6 ± 1.3 (98.6)[d]	62 ± 1.4 (100.3)[d]
Hyflon® AD60X	N_2	69.0 ± 2.8	68.2 ± 6.2	n.d.	n.d.
	O_2	131 ± 3.7	129.2 ± 10.7	n.d.	n.d.
	CO_2	78.1 ± 3.0	64.4 ± 1.7	70.8	79.0
	CH_4	20.9 ± 1.2	n.d.	17.8	18.6

[a] Data at 25 ± 1 °C obtained from the slope of the curves in Fig. 4E and F with Eq. (14). The indicated error is the standard deviation from the individually calculated diffusion coefficients for each thickness.
[b] Data at 23 ± 2 °C obtained from the fitting procedure described in Section 3.4 and Annexure C.
[c] Data at 17 ± 1 °C obtained from the slope of the curves in Fig. 4B and D.
[d] Values between parentheses are recalculated for 25 °C by the Arrhenius equation, using E_{d,CO_2} = 27.2 kJ mol^{-1} reported for Pebax [55] and estimating E_{d,CH_4} = 43.17 kJ mol^{-1}, reported for ABS [56], along with E_{d,CO_2} = 26.6 kJ mol^{-1} [56].

Nevertheless, even for these samples, the diffusion coefficient of the different gases can still be determined with reasonable accuracy from the slope of the curves by Eq. (17). The slope of CO_2 is higher for the vacuum operated system than for the sweeping gas system, but this is mainly a result of the lower measurement temperature and the diffusion coefficients correspond rather well after a temperature correction (Table 2).

As an independent method for the determination of the instrumental time lag, the permeation curve of an aluminium foil with a pinhole is analysed as well. For both instruments the aluminium sample accurately reproduces the instrumental time lag extrapolated from membranes with different thicknesses, and the flux follows Knudsen behaviour (SI Fig. 1). Flaconneche et al. who anticipated this method for determination of the diffusion coefficient [54], overlooked the necessity to introduce an instrumental time lag, correcting for the average residence time of the gases in the pipes, as discussed in Section 3.3.1 and implemented correctly in the present work. Instead, Watson and Baron use a slightly different setup, and determine the instrumental response from the pressure increase in the permeate chamber when a bypass valve to the pump is suddenly closed [24].

3.4. Calculation of diffusivities via simultaneous fitting procedure of all parameters

As shown in Fig. 8B and D, least squares fitting of the experimental data with Eq. (23) is somewhat sensitive to scatter in the individual data series. Therefore, slightly different values of the instrumental time lag are found for different gases and for different sets of polymers, in particular for the Hyflon® AD60X samples. Obviously, at constant temperature and pressure, the instrument-related parameters V_{Feed}, $V_{Downstream}$ and V_{Inlet} in Eq. (23) should be independent of the experimental conditions and the gas species. For very low permeation rates and high sweep flow rate, the sweep stream is essentially pure argon and thus also ϕ_{Inlet} and V_{Inlet}/ϕ_{Inlet} are constants. Thus, a calculation procedure was designed to fit all experimental data simultaneously with Eq. (23) against the independent variables ϕ_{Feed}, ϕ_{Sweep} and l^2, yielding the values of the instrumental parameters V_{Feed}, $V_{Downstream}$, V_{Inlet}/ϕ_{Inlet} and the diffusion coefficients D_i for each gas. Details of the procedure are given in Annexure C (Fig. 13). The results of the simultaneous fitting of the results of ca. 30 mixed gas permeation experiments as a function of the sweep flow rate for Pebax® 2533 and Hyflon® AD60X, and as a function of the feed flow rate for Pebax® 2533 are given in SI Figs. 3–5, respectively. The resulting values of the instrumental time lag, Θ_0, and the standard deviation of the individual time lags 21.0 ± 1.7 s for Pebax® 2533 and 23.8 ± 3.1 s for Hyflon® AD60X. The error of Pebax® 2533 is low enough for accurate determination of the instrumental time lag and, subsequently, of the diffusion coefficient in new membranes. On the other hand, the slight scatter in the Hyflon® AD60X data results in a relatively large error in the instrumental time lag. In this case, the variations in the Hyflon® AD60X results are most likely due to differences in the properties of the membranes due to residual solvent and the casting history. The variation in the results is an effective difference in the properties and not an experimental error in the determination of the time lag. Therefore, the method is reliable for any sample, but for further evaluation of unknown samples, it is best to rely on the instrumental time lag determined with Pebax® 2533 or with an aluminium film with pinhole defect. The calculated diffusion coefficients are listed in Table 2 and the values determined by the sweeping gas setup deviate less than 10% from the values determined by the fixed volume setup. This indicates in the first place the good accuracy of the method, and further confirms that for these two polymers no anomalous behaviour or significant coupling effect occurs at the given conditions, so that the pure and mixed gas diffusion coefficients are essentially the same. The diffusion coefficients obtained for CO_2 and CH_4 in Pebax® 2533 by the vacuum setup deviate around 23% from the values determined by the classical single gas time lag method. This difference is mostly due to the lower temperature in the vacuum-operated mixed gas instrument, operated at 17 °C. The values of Pebax were recalculated using the van't Hoff–Arrhenius equation:

$$D = D_0 \cdot e^{-\frac{E_d}{RT}} \quad (28)$$

After temperature correction, using the activation energy of diffusion, there is much better agreement of the values on vacuum-operated mixed gas setup with those of the other setups. The activation energy for CH_4 was not available but was estimated by that of ABS (Acrylonitrile-butadiene-styrene copolymer). This choice seems justified, given the very close resemblance of the activation energy reported for CO_2 in Pebax and in ABS (Table 2).

3.5. Validation experiments: effect of the CO_2 partial pressure on the CO_2/CH_4 mixed gas transport in the polymer of intrinsic microporosity PIM-EA-TB

In order to verify the developed method for materials with

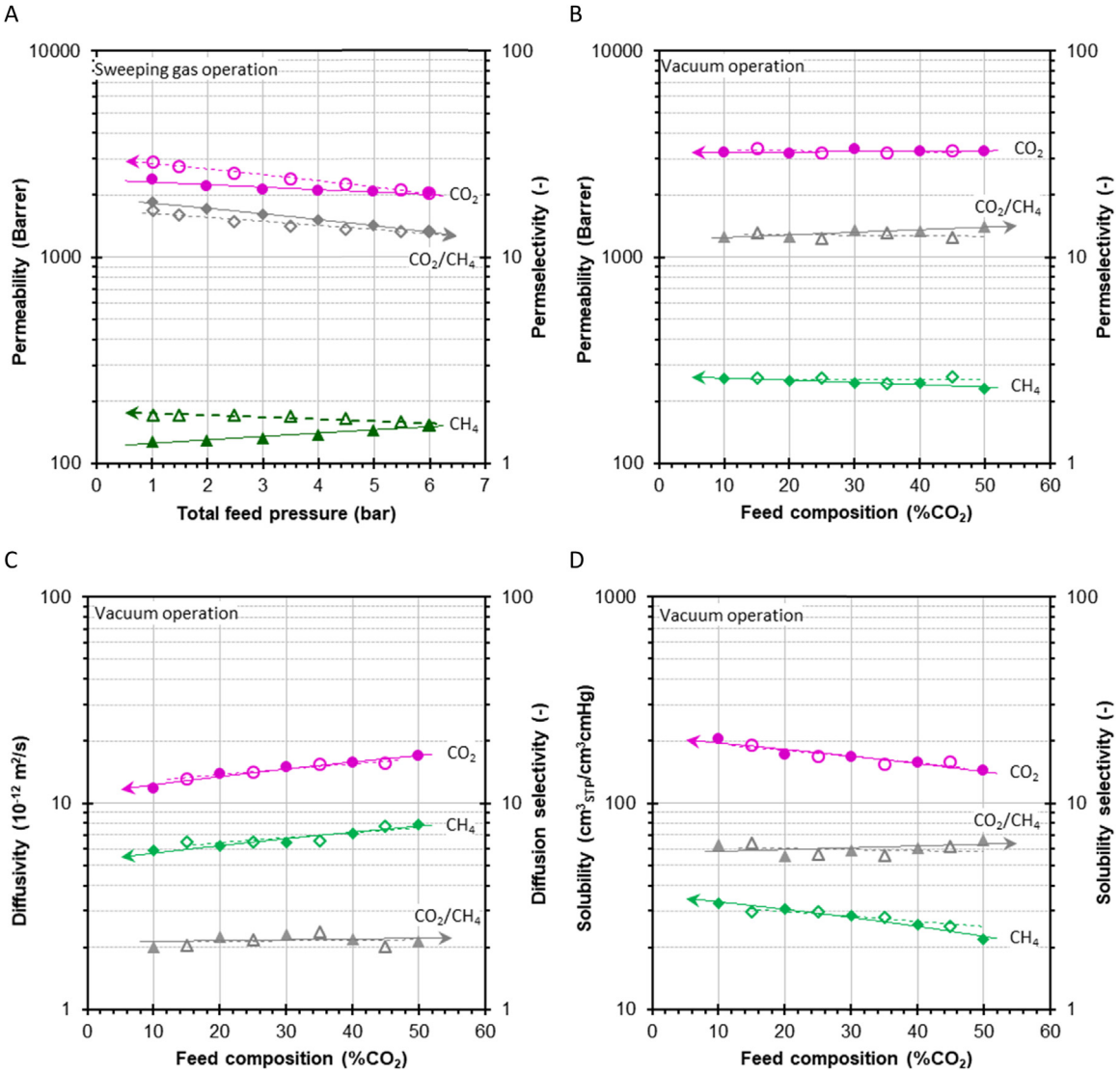

Fig. 9. Dependence of the mixed gas CO_2 and CH_4 permeability and selectivity of an aged sample PIM-EA-TB as a function of the total pressure in the sweeping gas setup (A) and as a function of the mixture composition in the vacuum setup (B) of sample PIM-EA-TB as a function of the gas mixture composition in the vacuum system. Sweeping gas system operating with mixture of 51/49 vol% CO_2/CH_4 in the pressure range from 1 to 6 bar(a) and vacuum system operating at a total feed pressure of 1.05 bar(a) and a composition in the range of 10–50 vol% CO_2. Concentration-dependence of CO_2 and CH_4 diffusivity and related selectivity (C) and indirectly calculated solubility (D). Filled symbols represent the runs with increasing pressure (A) or increasing CO_2 concentration (B–D) and open symbols represent the subsequently decreasing pressure or CO_2 concentration.

nonlinear sorption and transport behaviour, the permeation of CO_2/CH_4 gas mixtures in the polymer of intrinsic microporosity PIM-EA-TB [41,43] was studied. Fig. 9A shows a weak negative effect of the CO_2 partial pressure on the permeability coefficient of CO_2 both gases in an experiment with stepwise increase and decrease of the feed pressure (SI Fig. 6). In addition, this experiment shows weak hysteresis between the run with increasing CO_2 partial pressure (closed symbols) and subsequently decreasing CO_2 pressure (open symbols). This is due to CO_2 induced swelling of the aged matrix, leading to a slightly higher permeability and lower selectivity, as it also affects the CH_4 permeation. On the other hand, permeation of CO_2 in the CO_2/CH_4 mixture on the vacuum setup is nearly pressure-independent, probably because the total pressure in this experiment is only 1.05 bar and thus the methane concentration is considerably lower. Therefore, the present analysis is sufficiently accurate, whereas in the case of stronger pressure (and concentration) dependence, more complex approaches are needed to determine the transport parameters [57]. Remarkably, the CO_2 permeation curves on the vacuum setup show considerably faster permeation kinetics and thus a higher diffusion coefficient with increasing CO_2 concentration in the mixture (SI Fig. 1). The nearly pressure-independent permeability means that the increase in diffusivity (Fig. 9C) must be accompanied by decrease in the solubility (Fig. 9D). This is typical for PIMs, which usually have a strong dual mode sorption behaviour [58]. In the sweeping gas setup, the dual mode sorption behaviour affects CO_2 more than CH_4, causing a slight decrease in permselectivity with increasing pressure (Fig. 9A).

The results are in fair agreement with those reported previously for single gases [41], the differences being related to physical aging and to the mutual influence of the two gases in the membrane, either on the solubility or on the diffusivity, or both. The latter confirms the

importance of being able to measure not only the permeability but also the diffusion coefficient of gas mixtures.

4. Conclusions

A novel method to determine the diffusion coefficient of individual components of gas mixtures in polymeric membranes was developed. The method, based on online analysis of the permeate composition during the transient stage of permeation, is much more powerful than the traditional time lag method in a fixed volume setup because of its unique capacity to detect different gases simultaneously. Rapid sampling by online mass spectrometry of the permeate composition allows accurate determination of the transient behaviour.

The samples used for the method development were first fully characterized on the classical fixed volume time lag instrument. Calibration of the response of this instrument by two independent methods confirms its virtually negligible instrumental time lag of ca. 0.08 s, independent of the gas type. The first method measures the time lag directly from the permeation transient of different gases through an aluminium film with pinhole, and the second method extrapolates the time lag of polymer films with different thicknesses to zero thickness. This method also confirmed the thickness-independent properties of the Pebax test samples. In contrast, the same approach yields a finite instrumental time lag for the mixed gas permeation setup, which represents the average residence time of the gases in the setup between gas exposure of the membrane and detection of the gases by the mass spectrometer. Rubbery Pebax® 2533 was found to be more suitable than glassy Hyflon® AD60X for the method development and calibration of the instrumental parameters, requiring time- and history-independent membrane properties. Boundary conditions for accurate and reproducible determination of the mixed gas diffusion coefficients require that the time lag is independent of the permeation rate, and thus the latter must be negligible compared to the sweep flow rate. A low stage cut, by setting the feed flow rate much higher than the permeation rate, then guarantees that the measured transport properties only depend on the gas composition and pressure and not on other operation conditions.

The instrumental time lag depends on the flow rates, the gas pressure, and/or the pumping efficiency in the various parts of the system, and under the usual measurement conditions, it is approximately 20 s in the sweeping gas setup and approximately 10 s in the vacuum operated setup. After correction for the instrumental time lag, the novel method can determine the mixed gas diffusion coefficients with reasonably low error for any gas mixture and any polymeric membrane with an intrinsic time lag of some ten seconds and higher.

The first validation experiments on the polymer of intrinsic microporosity, PIM-EA-TB, not only demonstrate the success of the method, but show also the ability to detect the concentration and pressure dependency of the transport parameters, and other anomalous phenomena related to CO_2-induced dilation.

Finally, the method may easily be extended to step changes in the (partial) pressures during a running permeation experiment to study the effect of competitive sorption. The possibility to extend the studies to virtually any gas mixture, dry or humidified gases, or even gas-vapour mixtures, highlights its great potential for the investigation of mixed gas transport in polymeric membranes.

Acknowledgements

The work leading to these results has received funding from the European Union's Seventh Framework Program (*FP7/2007–2013*) under Grant agreement no. 608490, project M^4CO_2. This work was further supported by the CNR/FCT Italian/Portuguese Bilateral Project 2015–2016 “Advanced studies of the transport properties and gas separation by polymers of intrinsic microporosity (PIMs) and Ionic Liquid Gel Membranes via novel methods” and the CNR-CAS Bilateral Agreement 2016–2018 “Innovative polymeric membranes for pervaporation and advanced gas and vapour separations”.

Appendix A. Description of the time lag concept

The diffusion coefficient of the gases in the membranes was determined by the well-known time lag procedure, based on the penetration theory, and the instrument shown in Fig. 1. If a penetrant-free membrane is exposed to the penetrant at the feed side at $t = 0$ and the penetrant concentration is kept very low at the permeate side, then the total amount of penetrant, Q_t, passing through the membrane in time t is given by [17,18]:

$$\frac{Q_t}{l \cdot c_i} = \frac{D \cdot t}{l^2} - \frac{1}{6} - \frac{2}{\pi^2} \sum_1^\infty \frac{(-1)^n}{n^2} \exp\left(-\frac{D \cdot n^2 \cdot \pi^2 \cdot t}{l^2}\right) \tag{29}$$

in which c_i is the penetrant concentration at the membrane interface at the feed side, l is the membrane thickness (m) and D is the diffusion coefficient ($m^2\ s^{-1}$). For long periods of time the amount of permeant is given by:

$$Q_t = \frac{D \cdot c_i}{l} \cdot \left(t - \frac{l^2}{6D}\right) \tag{30}$$

For the fixed volume/pressure increase setup in the present work, Eq. (29) becomes:

$$p_t = \frac{RT \cdot A \cdot l}{V_P \cdot V_m} \cdot p_f \cdot S \times \left(\frac{D \cdot t}{l^2} - \frac{1}{6} - \frac{2}{\pi^2} \sum_1^\infty \frac{(-1)^n}{n^2} \exp\left(-\frac{D \cdot n^2 \cdot \pi^2 \cdot t}{l^2}\right)\right) \tag{31}$$

in which p_t is the permeate (bar) pressure at time t (s), R is the universal gas constant ($8.314 \cdot 10^{-5}\ m^3\ bar\ mol^{-1}\ K^{-1}$), T is the absolute temperature (K), A is the exposed membrane area (m^2), V_P is the permeate volume (m^3), V_m is the molar volume of a gas at standard temperature and pressure ($22.41 \cdot 10^{-3}\ m^3_{STP}\ mol^{-1}$ at 0 °C and 1 atm), p_f is the feed pressure (bar) and S is the gas solubility ($m^3_{STP}\ m^{-3}\ bar^{-1}$). At long times, the exponential term approaches to zero and Eq. (31) reduces to:

$$p_t = \frac{RT \cdot A \cdot l}{V_P \cdot V_m} \cdot p_f \cdot S\left(\frac{D \cdot t}{l^2} - \frac{1}{6}\right) = \frac{RT \cdot A}{V_P \cdot V_m} \cdot \frac{p_f \cdot S \cdot D}{l}\left(t - \frac{l^2}{6D}\right) \tag{32}$$

Thus, at long times a plot of p_t versus time describes a straight line which, upon extrapolation, intersects the time axis at $t = l^2/6D$, defined as the time lag, Θ (s).

$$\Theta = \frac{l^2}{6D} \tag{33}$$

With this equation, the diffusion coefficient can simply be obtained by time lag measurements if the membrane thickness is known. More complex systems require numerical methods or Laplace transformation to solve for the diffusion coefficient [59]. The permeability is determined from the steady state pressure increase rate:

$$P = \frac{V_P \cdot V_m \cdot l}{R \cdot T \cdot A \cdot p_f} \cdot \frac{dp}{dt} \tag{34}$$

In practice, for species with very low permeabilities the starting pressure and the baseline slope may not be completely negligible. The latter may be caused for instance by the formation of minor cracks in these rather brittle perfluoropolymers under the pressure of the sealing rings in the membrane cell. In that case Eqs. (31) and (32) must be redefined as:

$$p_t = p_0 + (dp/dt)_0 \cdot t + \frac{RT \cdot A \cdot l}{V_P \cdot V_m} \cdot p_f \cdot S \times \left(\frac{D \cdot t}{l^2} - \frac{1}{6} - \frac{2}{\pi^2} \sum_1^{\infty} \frac{(-1)^n}{n^2} \exp\left(-\frac{D \cdot n^2 \cdot \pi^2 \cdot t}{l^2} \right) \right) \tag{35}$$

$$p_t = p_0 + (dp/dt)_0 \cdot t + \frac{RT \cdot A}{V_P \cdot V_m} \cdot \frac{p_f \cdot S \cdot D}{l} \left(t - \frac{l^2}{6D} \right) \tag{36}$$

in which p_0 is the starting pressure (bar) and $(dp/dt)_0$ is the baseline slope (bar s^{-1}). Similar to what was described above, the time lag is then given by the intercept between the extrapolated baseline curve ($p_0 + t \cdot (dp/dt)_0$) and the steady state pressure increase curve. Thus, Eqs. (35) and (36) allow for the correct calculation of the solution, diffusion and permeability coefficients of any membrane, even in the case of minor defects, giving rise to some Knudsen-type diffusion and an apparent baseline drift.

Assuming the validity of the solution-diffusion model with pressure and concentration independent transport parameters, the solubility S (m^3_{STP} m^{-3} bar^{-1}) can be determined indirectly from the permeability and the diffusion coefficient by the simple relation:

$$S = \frac{P}{D} \tag{37}$$

Appendix B. Contribution of the tubes to the instrumental time lag

The flow regime in cylindrical tubes is determined by the Reynolds number, *Re*:

$$Re = \frac{\rho_i \cdot v \cdot d}{\eta_i} \tag{38}$$

where ρ_i is the density of the fluid (kg m^{-3}), v is the linear velocity (m s^{-1}), d is the tube diameter (m) and η_i is the fluid viscosity (Pa s). For $Re < 2000$, the flow regime is laminar and the pressure drop, dp/dx (Pa m^{-1}), is a function of the flow rate Q_i (m^3 s^{-1}).and given by:

$$\frac{dp}{dx} = 128 \frac{\eta_i \cdot Q_i}{\pi \cdot d^4} \tag{39}$$

Under all conditions (Fig. 10), the Reynolds number remains below 2000, which means that the flow is always in the laminar regime. The pressure drop is similar for all gases and is always negligible (below 1 mbar m^{-1} = 100 Pa m^{-1}) in tubes of 1/4″, but it rapidly increases in smaller tubes, to ca. 100–200 Pa m^{-1} at 200 ml min^{-1} for 1/8″ tubes and ca. 2000–3000 Pa m^{-1} at 200 ml min^{-1} for 1/16″ tubes. At the typical flow rate for the Argon sweep gas (30–50 cm^3 min^{-1}), the average residence time is in the order of 1–2 s m^{-1} in 1/16″ tubes, and this time increases rapidly to 4–7 s m^{-1} in 1/8″ tubes and to 15–25 s m^{-1} in 1/4″tubes (Fig. 11). This means that a suitable compromise must be sought between low pressure drop and acceptably low residence times, which do not contribute excessively to an instrumental time lag of the machine.

Experimental analysis of the influence of the feed flow rate and the sweep flow rate in the system operated under sweeping gas conditions:

As discussed above and in Section 3.3.1, each section of the instrument contributes to the overall time lag. An example of the importance of the individual contributions of the sweep flow in the setup with Argon sweep is shown in Fig. 12. At the sweep flow rate of 30 cm^3 min^{-1}, the downstream side of the setup contributes for approximately 6 s to the overall time lag. This contribution can be slightly reduced by setting the sweep flow rate higher, but this results in a lower permeate gas concentration. In any case, the sweep flow rate must be higher than the flow through the inlet capillary, which requires a minimum of approximately 11 cm^3 min^{-1} in the case of argon. As a compromise for optimum sensitivity and acceptably short residence times of the gas in the sweep line, the standard sweep flow rate is therefore set to 30 cm^3 min^{-1}.

In contrast to the feed and sweep flow rates, which are set by the user, the gas flow entering the analyser, ϕ_{Inlet}, depends on the gas itself and on conditions of the instrument. It might decrease in time in the case of contamination of the capillary or of the molecular leak in the injection system. Thus, the instrumental time lag must be checked periodically. Since the inlet flow depends on the gas type, it is important to keep the composition of the gas to be analysed as constant as possible, i.e., the sweep flow rate should be much higher than the permeate flow rate.

The slope of the curves in Fig. 12A and B corresponds to the dead volume of the permeate side. Simultaneous fitting of the data for different gases yields a volume of 2.2 cm^3 for the feed side and 3.1 cm^3 for the permeate side (Annexure C). This means that at feed flow rate of 200 cm^3 min^{-1} and a sweep flow rate of 30 cm^3 min^{-1} they are responsible for 0.66 s and 6.1 s of the instrumental time lag, respectively. This means that the remaining part of the instrumental time lag is due to the transport of the gas from the sampling point through the 6-valve port and the capillary into the MS, which accounts for approximately 13 s and thus forms the largest contribution.

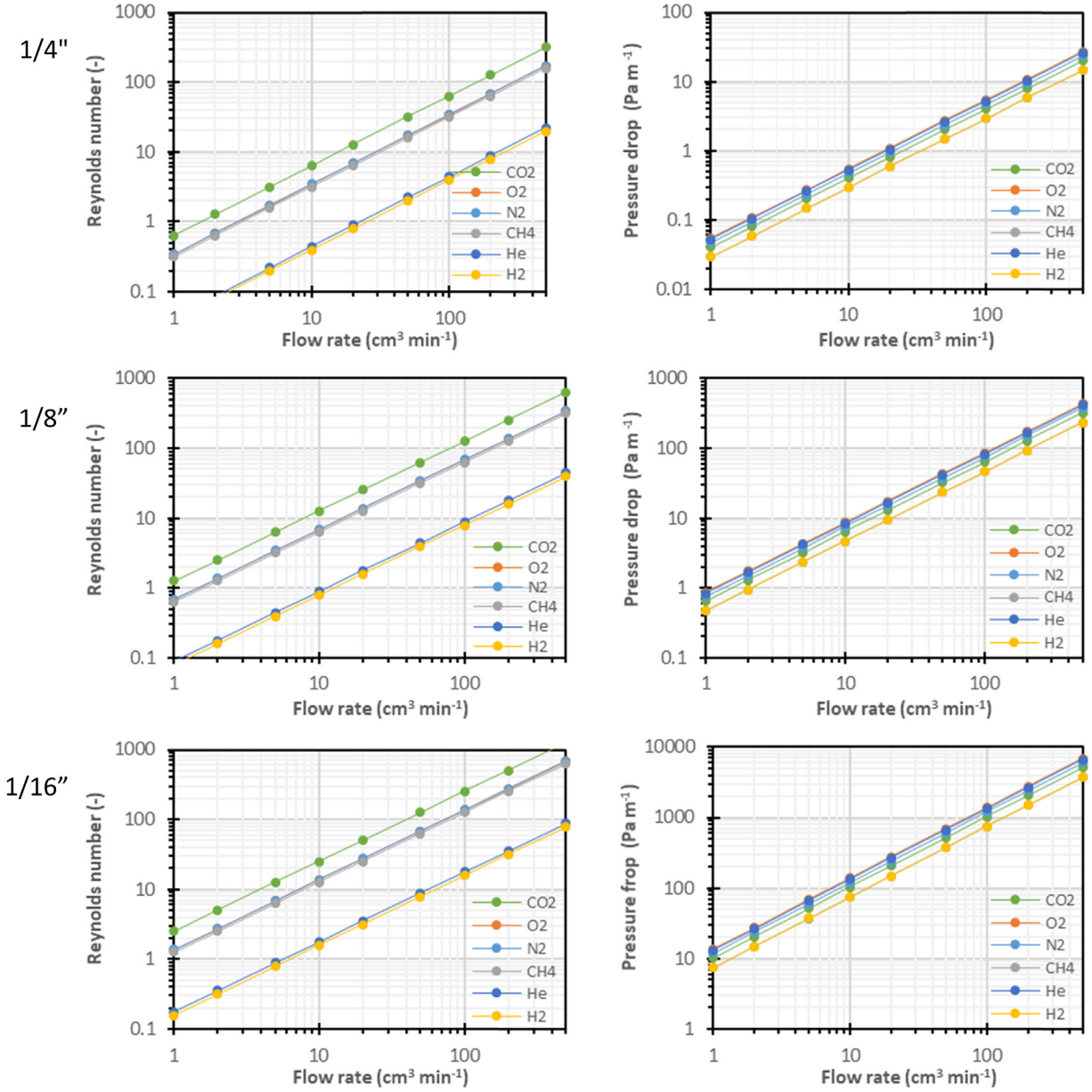

Fig. 10. Reynolds number (left) and pressure drop (right) in of tubes of different diameters for six light gases at typical flow rates in permeation experiments.

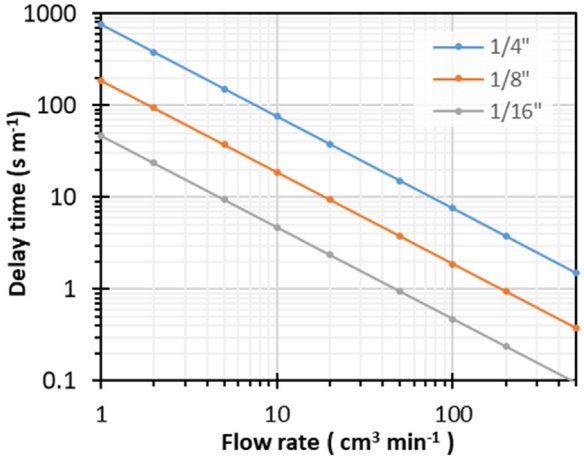

Fig. 11. Approximate residence time of the gas as a function of the volumetric gas flow rate in tubes of different diameter.

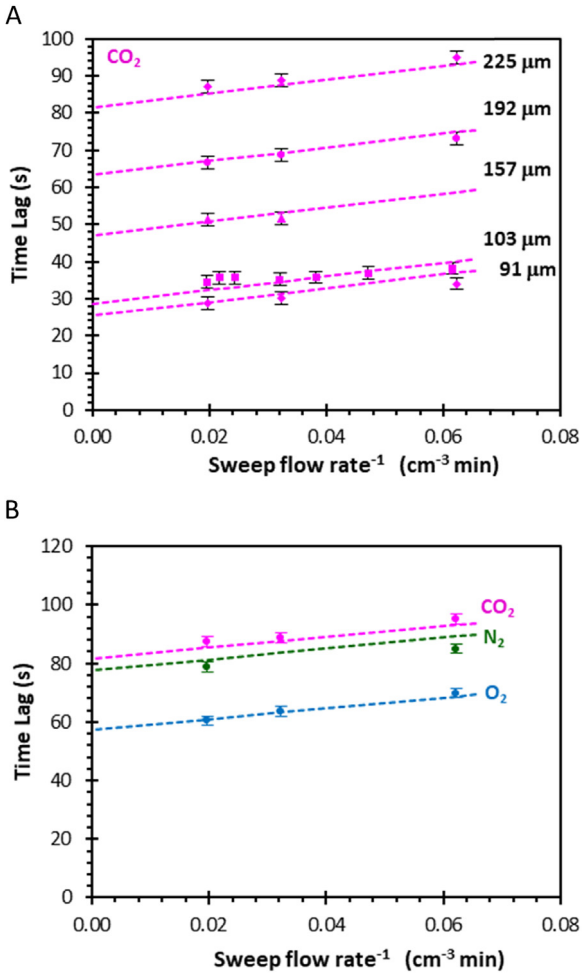

Fig. 12. A) Typical examples of the dependence of the time lag on the reciprocal sweep flow rate $1/\phi_{Sweep}$ for CO_2 in five membranes with different thickness, and B) the reciprocal sweep flow rate for the three gases in the 225 µm thick Pebax® 2533 membrane for the sweeping gas setup. Dashed lines and error bars represent the fit and the standard deviation of the simultaneous fit of all parameters by the procedure mentioned in Annexure C.

Appendix C. Least squares fitting procedure with error analysis for simultaneous calculation of the diffusion coefficient from all measurements

Details of the method described in Section 3.4 are as follows: for every given membrane with thickness l, and at a given feed flow rate ϕ_{Feed} and sweep flow rate ϕ_{Sweep}, the time lag was calculated as

$$\Theta_{i,calc} = \frac{V_{Feed,Fit}}{\phi_{Feed}} + \frac{V_{Perm,Fit}}{\phi_{Sweep}} + \left(\frac{V_{Inlet}}{\phi_{Inlet}}\right)_{Fit} + \frac{l^2}{6D_{i,Fit}} \tag{40}$$

where $V_{Feed,Fit}$, $V_{Perm,Fit}$, $\left(\frac{V_{Inlet}}{\phi_{Inlet}}\right)_{Fit}$ and $D_{i,Fit}$ are estimated fit parameters. After a first estimation of these parameters, the sum of the squared error is calculated for all measurements j *(on a total of x)* and all gases i as:

$$\sum Err^2 = \sum_{j=1}^{x}\left(\sum_i (\Theta_{i,calc} - \Theta_{i,\exp})^2\right)_j \tag{41}$$

Minimization of this term by a standard Excel routine gives the values for the time lag and the diffusion coefficient for all gases.

For a statistical analysis of the validity of this method, the absolute error, $\Delta\Theta_i$, in the determination of the time lag for each gas i in every measurement j, and the average absolute error for all measurements, $\delta\Theta_i$, were calculated as:

$$\Delta\Theta_i = |\Theta_{i,calc} - \Theta_{i,\exp}| \tag{42}$$

$$\delta\Theta_i = \frac{1}{n}\sum_{j=1}^{x}\sum_i \Delta\Theta_i = \frac{1}{n}\sum_{j=1}^{x}\sum_i |\Theta_{i,calc} - \Theta_{i,\exp}|_j \tag{43}$$

where x is the total number of analyses carried out and n is the total number of results. The standard error of the model (i.e. the standard error of the regression) for a line with slope and intercept, $\sigma\Theta_i$, is:

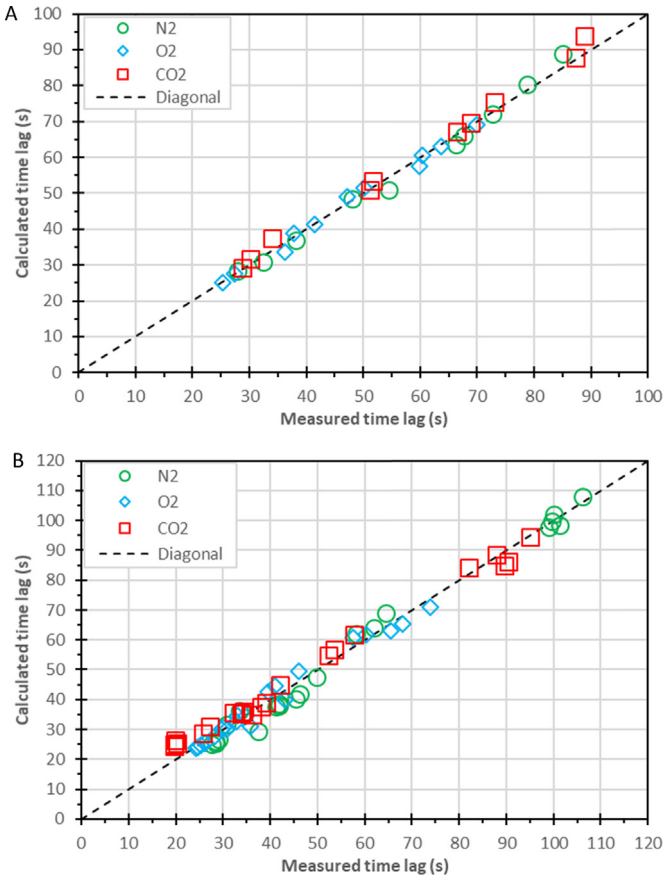

Fig. 13. Plot of the calculated time lag versus the experimental time lag for Pebax® 2533 (top) and for Hyflon® AD60X (bottom) for N_2, O_2 and CO_2 in the mixture 80/10/10 vol%. The corresponding values of $\delta\Theta_i$, were 1.46 s for Pebax® 2533, and 2.46 s for Hyflon® AD60X.

Table 3
Results of the simultaneous fitting procedure of the instrumental parameters and diffusion coefficients by the sweeping gas setup.

Pebax® 2533	**Hyflon® AD60X**
$V_{perm\_calc} = 3.03\ cm^3$	$V_{perm\_calc} = 2.72\ cm^3$
$\Theta'_0 = 14.92\ s$	$\Theta'_0 = 18.44\ s$
Θ_0 @ 30 $cm^3\ min^{-1}$ Ar = 20.99 ± 1.70[a] s	Θ_0 @ 30 $cm^3\ min^{-1}$ Ar = 23.88 ± 3.13[a] s
$D(O_2) = 199.0 \times 10^{-12}\ m^2\ s^{-1}$	$D(O_2) = 127.1 \times 10^{-12}\ m^2\ s^{-1}$
$D(N_2) = 135.7 \times 10^{-12}\ m^2\ s^{-1}$	$D(N_2) = 65.6 \times 10^{-12}\ m^2\ s^{-1}$
$D(CO_2) = 125.7 \times 10^{-12}\ m^2\ s^{-1}$	$D(CO_2) = 79.8 \times 10^{-12}\ m^2\ s^{-1}$

[a] Standard error calculated by Eq. (44).

$$\sigma\Theta_i = \sqrt{\frac{1}{n-2}\sum Err^2} = \sqrt{\frac{1}{n-2}\sum_{j=1}^{x}\left(\sum_i (\Theta_{i,calc} - \Theta_{i,\exp})^2\right)_j} \quad (44)$$

where (n − 2) represents the degrees of freedom of the model and 2 is the number of parameters (slope and intercept). For simultaneous fitting of multiple parameters, the degrees of freedom decrease accordingly. The correlation of the experimental and calculated data is shown in Fig. 13. The absolute average error in the time lag, $\delta\Theta_i$, calculated for Pebax® 2533 equals 1.36 s (standard error = 1.70 s) and for Hyflon® AD60X membranes it is 2.46 s (standard error = 3.13 s).

Given the average error in the instrumental time lag determined with the Pebax samples, the accuracy in the determination of the diffusion coefficient becomes acceptable if the membrane time lag is some tens of seconds or higher, resulting in less than 10% error in the analysis. The quantitative fitting parameters are given in Table 3 and show that the dead volume at the permeate side of the membrane is approximately 3 cm^3, which contributes to approximately 6 s of the total instrumental time lag at 30 $cm^3\ min^{-1}$ sweep flow rate. The plot of the fitted cures, along with the experimental data, are given in the Supplementary information (SI Figs. 3–5).

Appendix D. Supplementary material

Supplementary data associated with this article can be found in the online version at http://dx.doi.org/10.1016/j.memsci.2018.04.029.

References

[1] W.J. Koros, A. Kratochvil, S. Shu, S. Husain, Energy and Environmental Issues and Impacts of Membranes in Industry, (2009), http://dx.doi.org/10.1002/9783527626779.ch7.

[2] H.B. Park, J. Kamcev, L.M. Robeson, M. Elimelech, B.D. Freeman, Maximizing the right stuff: the trade-off between membrane permeability and selectivity, Science 356 (2017) eaab0530, http://dx.doi.org/10.1126/science.aab0530 (80-.).

[3] I. Pinnau, L.G. Toy, Gas and vapor transport properties of amorphous perfluorinated copolymer membranes based on 2,2-bistrifluoromethyl-4,5-difluoro-1,3-dioxole/tetrafluoroethylene, J. Memb. Sci. 109 (1996) 125–133, http://dx.doi.org/10.1016/0376-7388(95)00193-X.

[4] R.R. Tiwari, Z.P. Smith, H. Lin, B.D. Freeman, D.R. Paul, Gas permeation in thin films of "high free-volume" glassy perfluoropolymers: Part I. Physical aging, Polymer 55 (2014) 5788–5800, http://dx.doi.org/10.1016/j.polymer.2014.09.022.

[5] Z. Cui, E. Drioli, Y.M. Lee, Recent progress in fluoropolymers for membranes, Prog. Polym. Sci. 39 (2014) 164–198, http://dx.doi.org/10.1016/j.progpolymsci.2013.07.008.

[6] N.B. McKeown, P.M. Budd, K.J. Msayib, B.S. Ghanem, H.J. Kingston, C.E. Tattershall, S. Makhseed, K.J. Reynolds, D. Fritsch, Polymers of intrinsic microporosity (PIMs): bridging the void between microporous and polymeric materials, Chem. – Eur. J. 11 (2005) 2610–2620, http://dx.doi.org/10.1002/chem.200400860.

[7] N.B. McKeown, P.M. Budd, Polymers of intrinsic microporosity (PIMs): organic materials for membrane separations, heterogeneous catalysis and hydrogen storage, Chem. Soc. Rev. 35 (2006) 675–683, http://dx.doi.org/10.1039/b600349d.

[8] I. Rose, C.G. Bezzu, M. Carta, B. Comesaña-Gándara, E. Lasseuguette, M.C.C. Ferrari, P. Bernardo, G. Clarizia, A. Fuoco, J.C. Jansen, K.E.E. Hart, T.P. Liyana-Arachchi, C.M. Colina, N.B. McKeown, Polymer ultrapermeability from the inefficient packing of 2D chains, Nat. Mater. 16 (2017) 932–937, http://dx.doi.org/10.1038/nmat4939.

[9] S. Thomas, I. Pinnau, N. Du, M.D. Guiver, Pure- and mixed-gas permeation properties of a microporous spirobisindane-based ladder polymer (PIM-1), J. Memb. Sci. 333 (2009) 125–131, http://dx.doi.org/10.1016/j.memsci.2009.02.003.

[10] N. Du, H.B. Park, G.P. Robertson, M.M. Dal-Cin, T. Visser, L. Scoles, M.D. Guiver, Polymer nanosieve membranes for CO_2-capture applications, Nat. Mater. 10 (2011) 372–375, http://dx.doi.org/10.1038/nmat2989.

[11] H.B. Park, C.H. Jung, Y.M. Lee, A.J. Hill, S.J. Pas, S.T. Mudie, E. Van Wagner, B.D. Freeman, D.J. Cookson, Polymers with cavities tuned for fast selective transport of small molecules and ions, Science 318 (2007) 254–258, http://dx.doi.org/10.1126/science.1146744.

[12] H.B. Park, S.H. Han, C.H. Jung, Y.M. Lee, A.J. Hill, Thermally rearranged (TR) polymer membranes for CO_2 separation, J. Memb. Sci. 359 (2010) 11–24, http://dx.doi.org/10.1016/j.memsci.2009.09.037.

[13] H. Shamsipur, B.A. Dawood, P.M. Budd, P. Bernardo, G. Clarizia, J.C. Jansen, Thermally rearrangeable PIM-polyimides for gas separation membranes, Macromolecules 47 (2014) 5595–5606, http://dx.doi.org/10.1021/ma5011183.

[14] J.E. Bara, T.K. Carlisle, C.J. Gabriel, D. Camper, A. Finotello, D.L. Gin, R.D. Noble, Guide to CO_2 separations in imidazolium-based room-temperature ionic liquids, Ind. Eng. Chem. Res. 48 (2009) 2739–2751, http://dx.doi.org/10.1021/ie8016237.

[15] J.C. Jansen, K. Friess, G. Clarizia, J. Schauer, P. Izák, High ionic liquid content polymeric gel membranes: preparation and performance, Macromolecules 44 (2011) 39–45, http://dx.doi.org/10.1021/ma102438k.

[16] Z. Dai, R.D. Noble, D.L. Gin, X. Zhang, L. Deng, Combination of ionic liquids with membrane technology: a new approach for CO_2 separation, J. Memb. Sci. 497 (2016) 1–20, http://dx.doi.org/10.1016/j.memsci.2015.08.060.

[17] J. Crank, The Mathematics of Diffusion, 2nd ed, Clarendon Press, Oxford, 1975〈https://books.google.it/books/about/The_mathematics_of_diffusion.html?id=7QjwAAAAMAAJ&redir_esc=y〉.

[18] J. Crank, G.S. Park, Diffusion in Polymers, Academic Press, London, New York, 1968〈https://books.google.it/books?id=TJkpcAAACAAJ〉.

[19] S.W. Rutherford, D.D. Do, Review of time lag permeation technique as a method for characterisation of porous media and membranes, Adsorption 3 (1997) 283–312, http://dx.doi.org/10.1007/BF01653631.

[20] M.C. Villet, G.R. Gavalas, Measurement of concentration-dependent gas diffusion coefficients in membranes from a psuedo-steady state permeation run, J. Memb. Sci. 297 (2007) 199–205, http://dx.doi.org/10.1016/j.memsci.2007.03.045.

[21] N. Al-Qasas, J. Thibault, B. Kruczek, A new characterization method of membranes with nonlinear sorption isotherm systems based on continuous upstream and downstream time-lag measurements, J. Memb. Sci. 542 (2017) 91–101, http://dx.doi.org/10.1016/j.memsci.2017.07.039.

[22] J.C. Jansen, K. Friess, E. Tocci, M. Macchione, Amorphous glassy perfluoropolymer membranes of Hyflon AD®: free volume distribution by photochromic probing and vapour transport properties, in: Y. Yampolskii, B. Freeman (Eds.), Membr. Gas Sep. John Wiley & Sons, Ltd., Chichester, UK, 2010, pp. 59–83, , http://dx.doi.org/10.1002/9780470665626.ch4.

[23] J.C. Jansen, K. Friess, E. Drioli, Organic vapour transport in glassy perfluoropolymer membranes: a simple semi-quantitative approach to analyze clustering phenomena by time lag measurements, J. Memb. Sci. 367 (2011) 141–151, http://dx.doi.org/10.1016/j.memsci.2010.10.063.

[24] J.M. Watson, M.G. Baron, Precise static and dynamic permeation measurements using a continuous-flow vacuum cell, J. Memb. Sci. 106 (1995) 259–268, http://dx.doi.org/10.1016/0376-7388(95)00090-Y.

[25] R.D. Raharjo, B.D. Freeman, E.S. Sanders, Pure and mixed gas CH_4 and n-C_4H_{10} sorption and dilation in poly(dimethylsiloxane), J. Memb. Sci. 292 (2007) 45–61, http://dx.doi.org/10.1016/j.memsci.2007.01.012.

[26] O. Vopička, M.G. De Angelis, G.C. Sarti, Mixed gas sorption in glassy polymeric membranes: I. CO_2/CH4 and n-C_4/CH_4 mixtures sorption in poly(1-trimethylsilyl-1-propyne) (PTMSP), J. Memb. Sci. 449 (2014) 97–108, http://dx.doi.org/10.1016/j.memsci.2013.06.065.

[27] O. Vopička, M.G. De Angelis, N. Du, N. Li, M.D. Guiver, G.C. Sarti, Mixed gas sorption in glassy polymeric membranes: II. CO_2/CH4 mixtures in a polymer of intrinsic microporosity (PIM-1), J. Memb. Sci. 459 (2014) 264–276, http://dx.doi.org/10.1016/j.memsci.2014.02.003.

[28] L. Garrido, C. García, M. López-González, B. Comesaña-Gándara, Á.E. Lozano, J. Guzmán, Determination of gas transport coefficients of mixed gases in 6FDA-TMPDA polyimide by NMR spectroscopy, Macromolecules 50 (2017) 3590–3597, http://dx.doi.org/10.1021/acs.macromol.7b00384.

[29] J. Chen, L. Loo, K. Wang, A. Novel, Time lag method to measure the permeation of vapor-gas mixtures, J. Membr. Sep. Technol. 1 (2012) 94–99, http://dx.doi.org/10.6000/1929-6037.2012.01.02.3.

[30] K.D. Cook, K.H. Bennett, M.L. Haddix, On-line mass spectrometry: a faster route to process monitoring and control, Ind. Eng. Chem. Res. 38 (1999) 1192–1204, http://dx.doi.org/10.1021/ie9707984.

[31] S.L. Shannon, J.G. Goodwin, Characterization of catalytic surfaces, Chem. Rev. 95 (1995) 677–695, http://dx.doi.org/10.1021/cr00035a011.

[32] R.C. Johnson, R.G. Cooks, T.M. Allen, M.E. Cisper, P.H. Hemberger, Membrane introduction mass spectrometry: trends and applications, Mass Spectrom. Rev. 19 (2000) 1–37, http://dx.doi.org/10.1002/(SICI)1098-2787(2000)19:1<1::AID-MAS1>3.0.CO;2-Y.

[33] P.D. Tortell, Dissolved gas measurements in oceanic waters made by membrane inlet mass spectrometry, Limnol. Oceanogr. Methods 3 (2005) 24–37, http://dx.doi.org/10.4319/lom.2005.3.24.

[34] T. Schäfer, J. Vital, J.G. Crespo, Coupled pervaporation/mass spectrometry for investigating membrane mass transport phenomena, J. Memb. Sci. 241 (2004) 197–205, http://dx.doi.org/10.1016/j.memsci.2004.05.014.

[35] Z. Zhang, R. Chattot, L. Bonorand, K. Jetsrisuparb, Y. Buchmüller, A. Wokaun, L. Gubler, Mass spectrometry to quantify and compare the gas barrier properties of radiation grafted membranes and Nafion®, J. Memb. Sci. 472 (2014) 55–66, http://dx.doi.org/10.1016/j.memsci.2014.08.020.

[36] K. Tanaka, H. Kita, K.I. Okamoto, R.D. Noble, J.L. Falconer, Isotopic-transient permeation measurements in steady-state pervaporation through polymeric membranes, J. Memb. Sci. 197 (2002) 173–183, http://dx.doi.org/10.1016/S0376-7388(01)00636-6.

[37] C. Brazinha, A.P. Fonseca, O.M.N.D. Teodoro, J.G. Crespo, On-line and real-time monitoring of organophilic pervaporation by mass spectrometry, J. Memb. Sci. 347 (2010) 83–92, http://dx.doi.org/10.1016/j.memsci.2009.10.009.

[38] S.C. Fraga, L. Trabucho, C. Brazinha, J.G. Crespo, Characterisation and modelling of transient transport through dense membranes using on-line mass spectrometry, J. Memb. Sci. 479 (2015) 213–222, http://dx.doi.org/10.1016/j.memsci.2014.12.016.

[39] P. Tremblay, M.M. Savard, J. Vermette, R. Paquin, Gas permeability, diffusivity and solubility of nitrogen, helium, methane, carbon dioxide and formaldehyde in dense polymeric membranes using a new on-line permeation apparatus, J. Memb. Sci. 282 (2006) 245–256, http://dx.doi.org/10.1016/j.memsci.2006.05.030.

[40] K. Pilnacek, J.C. Jansen, P. Bernardo, G. Clarizia, F. Bazzarelli, F. Tasselli, Determination of mixed gas permeability of high free volume polymers using direct mass spectrometric analysis of the gas compositions, Procedia Eng. (2012) 1027–1029, http://dx.doi.org/10.1016/j.proeng.2012.08.664.

[41] M. Carta, R. Malpass-Evans, M. Croad, Y. Rogan, J.C. Jansen, P. Bernardo, F. Bazzarelli, N.B. McKeown, An efficient polymer molecular sieve for membrane gas separations, Science 339 (80-.) (2013) 303–307, http://dx.doi.org/10.1126/science.1228032.

[42] M.R. Khdhayyer, E. Esposito, A. Fuoco, M. Monteleone, L. Giorno, J.C. Jansen, M.P. Attfield, P.M. Budd, Mixed matrix membranes based on UiO-66 MOFs in the polymer of intrinsic microporosity PIM-1, Sep. Purif. Technol. 173 (2017) 304–313, http://dx.doi.org/10.1016/j.seppur.2016.09.036.

[43] E. Tocci, L. De Lorenzo, P. Bernardo, G. Clarizia, F. Bazzarelli, N.B. McKeown, M. Carta, R. Malpass-Evans, K. Friess, K. Pilnáček, M. Lanč, Y.P. Yampolskii, L. Strarannikova, V. Shantarovich, M. Mauri, J.C. Jansen, Molecular modeling and gas permeation properties of a polymer of intrinsic microporosity composed of ethanoanthracene and Tröger's base units, Macromolecules 47 (2014) 7900–7916, http://dx.doi.org/10.1021/ma501469m.

[44] S.C. Fraga, M.A. Azevedo, I.M. Coelhoso, C. Brazinha, J.G. Crespo, Steady-state and transient transport studies of gas permeation through dense membranes using on-line mass spectrometry, Sep. Purif. Technol. 197 (2018) 18–26, http://dx.doi.org/10.1016/j.seppur.2017.12.026.

[45] K. Pilnáček, O. Vopička, M. Lanč, M. Dendisová, M. Zgažar, P.M. Budd, M. Carta, R. Malpass-Evans, N.B. McKeown, K. Friess, Aging of polymers of intrinsic microporosity tracked by methanol vapour permeation, J. Memb. Sci. 520 (2016) 895–906, http://dx.doi.org/10.1016/j.memsci.2016.08.054.

[46] P. Bernardo, F. Bazzarelli, F. Tasselli, G. Clarizia, C.R. Mason, L. Maynard-Atem, P.M. Budd, M. Lanč, K. Pilnáček, O. Vopička, K. Friess, D. Fritsch, Y.P. Yampolskii, V. Shantarovich, J.C. Jansen, Effect of physical aging on the gas transport and sorption in PIM-1 membranes, Polymer 113 (2017) 283–294, http://dx.doi.org/10.1016/J.POLYMER.2016.10.040.

[47] J.C. Jansen, M. Macchione, E. Drioli, On the unusual solvent retention and the effect on the gas transport in perfluorinated Hyflon AD® membranes, J. Memb. Sci. 287 (2007) 132–137, http://dx.doi.org/10.1016/j.memsci.2006.10.031.

[48] M. Macchione, J.C. Jansen, G. De Luca, E. Tocci, M. Longeri, E. Drioli, Experimental analysis and simulation of the gas transport in dense Hyflon® AD60X membranes:

influence of residual solvent, Polymer 48 (2007) 2619–2635, http://dx.doi.org/10.1016/j.polymer.2007.02.068.
[49] P. Bernardo, J.C. Jansen, F. Bazzarelli, F. Tasselli, A. Fuoco, K. Friess, P. Izák, V. Jarmarová, M. Kačírková, G. Clarizia, Gas transport properties of Pebax®/room temperature ionic liquid gel membranes, Sep. Purif. Technol. 97 (2012) 73–82, http://dx.doi.org/10.1016/j.seppur.2012.02.041.
[50] H. Ørsnes, S. Bohatka, H. Degn, Reaction of water at hot filament interferes with measurements of dissolved gases by membrane inlet mass spectrometry, Rapid Commun. Mass Spectrom. 11 (1997) 1736–1738, http://dx.doi.org/10.1002/(SICI)1097-0231(19971015)11:15<1736::AID-RCM50>3.0.CO;2-J.
[51] M. Al-Ismaily, J.G. Wijmans, B. Kruczek, A shortcut method for faster determination of permeability coefficient from time lag experiments, J. Memb. Sci. 423–424 (2012) 165–174, http://dx.doi.org/10.1016/J.MEMSCI.2012.08.009.
[52] C.R. Lieszkovszky, L. Filippelli, A.R. Tilford, Metrological characteristics of a group of quadrupole partial pressure analyzers, J. Vac. Sci. Technol. A Vac. Surf. Films 8 (1990) 3838–3854, http://dx.doi.org/10.1116/1.576458.
[53] J.A. Basford, M.D. Boeckmann, R.E. Ellefson, A.R. Filippelli, D.H. Holkeboer, L. Lieszkovsky, C.M. Stupak, Recommended practice for the calibration of mass spectrometers for partial pressure analysis, J. Vac. Sci. Technol. A Vac. Surf. Films A11 (1993) A22, http://dx.doi.org/10.1116/1.4755937.
[54] B. Flaconneche, J. Martin, M.H. Klopffer, Transport properties of gases in polymers: experimental methods, Oil Gas Sci. Technol. 56 (2001) 245–259, http://dx.doi.org/10.2516/ogst:2001022.
[55] J.H. Kim, S.Y. Ha, Y.M. Lee, Gas permeation of poly(amide-6-b-ethylene oxide) copolymer, J. Memb. Sci. 190 (2001) 179–193, http://dx.doi.org/10.1016/S0376-7388(01)00444-6.
[56] J. Marchese, E. Garis, M. Anson, N.A. Ochoa, C. Pagliero, Gas sorption, permeation and separation of ABS copolymer membrane, J. Memb. Sci. 221 (2003) 185–197, http://dx.doi.org/10.1016/S0376-7388(03)00258-8.
[57] P. Borys, A. Rybak, Z.J. Grzywna, On the analysis of concentration-dependent diffusion using transient sorption and permeation measurements by the D1–D8 system, Ind. Eng. Chem. Res. 52 (2013) 8887–8896, http://dx.doi.org/10.1021/ie302333d.
[58] P. Li, T.S. Chung, D.R. Paul, Temperature dependence of gas sorption and permeation in PIM-1, J. Memb. Sci. 450 (2014) 380–388, http://dx.doi.org/10.1016/j.memsci.2013.09.030.
[59] P. Taveira, A. Mendes, C. Costa, On the determination of diffusivity and sorption coefficients using different time-lag models, J. Memb. Sci. 221 (2003) 123–133, http://dx.doi.org/10.1016/S0376-7388(03)00252-7.